REPORT DOCUMENTATION PAGE

AFRL-SR-AR-TR-03-

0316

1. REPORT DATE	2. REPORT TYPE	3. DATES COVERED (From - To)
7/16/03	Final Technical Report	01 May 99-30 Apr 03

4. TITLE AND SUBTITLE:

DEPSCoR 99 PERCUTANEOUS ABSORPTION, SKIN BIOPHYSICS AND DERMATOTOXICITY FROM JP-8

5a. CONTRACT NUMBER

5b. GRANT NUMBER
F49620-99-1-0223

5c. PROGRAM ELEMENT NUMBER

6. AUTHOR(S)

Jagdish Singh

5d. PROJECT NUMBER

5e. TASK NUMBER

5f. WORK UNIT NUMBER

7. PERFORMING ORGANIZATION NAME(S) AND ADDRESS(ES)

North Dakota State University
P.O. Box 5790
Fargo, ND 58105

8. PERFORMING ORGANIZATION REPORT NUMBER

Fourth and final report

9. SPONSORING / MONITORING AGENCY NAME(S) AND ADDRESS(ES)
AFOSR/NL
801 N. Randolph St. Room 732
Arlington VA 22203-1977

10. SPONSOR/MONITOR'S ACRONYM(S)
AFOSR/PK2

11. SPONSOR/MONITOR'S REPORT NUMBER(S)

12. DISTRIBUTION / AVAILABILITY STATEMENT

Approve for Public Release: Distribution Unlimited.

20030915 025

13. SUPPLEMENTARY NOTES

14. ABSTRACT: JP-8 and its major aromatic and aliphatic components were investigated for percutaneous absorption and dermal toxicity in vitro and in vivo. *In vitro* studies showed SC lipid and protein extraction, macroscopic barrier perturbation, and microscopic changes in JP-8 treated skin samples. Transmission electron micrograph showed many ultrastructural modifications in JP-8 treated porcine skin namely expansion in the intercellular spaces of stratum corneum, reduction in compactness of tonofibrils of stratum spinosum, altered configuration and disrupted attachment of basale cells, reduction in dendritic processes of Langerhans' cells. In *in vitro* studies with JP-8 components, tridecane exhibited greater permeability through skin among aliphatic and naphthalene among aromatic JP-8 components, which may be due to their greater diffusion through skin. All of the chemicals caused significant ($p < 0.05$) increase in TEWL values through skin. This indicates potential skin irritation and dermatotoxicity by JP-8 components. Amount of chemicals absorbed suggests that tridecane among aliphatic components and, naphthalene and its methyl derivatives among aromatic components should be monitored for their possible systemic toxicity. *In vivo* studies with JP-8 and its model components in rabbit showed an increase in temperature, capacitance, TEWL and severe to moderate erythema and edema with all test chemicals. The quantitative microscopic measurement results showed increase in epidermal thickness, and decrease in collagen fibers' bundle length and thickness. This constitutes potential dermatotoxicity from these chemicals. The DEPSCoR funding also allowed us to provide research experience to a research associate, a graduate student, and two undergraduate students in the area of percutaneous absorption and dermal toxicity from JP-8 and its major components and led to six publications in peer-reviewed journals and ten presentations in national/international symposia and seminars.

15. SUBJECT TERMS

16. SECURITY CLASSIFICATION OF:			17. LIMITATION OF ABSTRACT	18. NUMBER OF PAGES	19a. NAME OF RESPONSIBLE PERSON
a. REPORT	b. ABSTRACT	c. THIS PAGE			Jagdish Singh
					19b. TELEPHONE NUMBER *(include area code)* (701) 231-7943

FINAL TECHNICAL REPORT

DEPSCoR 99 Percutaneous Absorption, Skin Biophysics, and Dermatotoxicity from JP-8 jet fuel
Grant Number # F49620-99-1-0223
Program manager # Dr. Walter Kozumbo, NL (703) 696-7720
Principal Investifator: Dr. Jagdish Singh

Abstract: JP-8 is kerosene based multicomponent mixture of aromatic and aliphatic hydrocarbons, without the lower molecular weight fractions. Both military and commercial aircraft workers are at risk of dermal exposure and toxicity from JP-8 jet fuel. Quantitation of penetration of chemicals through skin is necessary for assessment of health hazards involved in these occupational environments. We investigated the following specific aims: (A). To determine percutaneous absorption of dodecane, tridecane, tetradecane, naphthalene, 1-methylnaphthalene, and 2-methylnaphthalene *in vitro* through dermatomed skin using Franz diffusion cells. (B). To study the binding of these chemicals to the stratum corneum (SC). (C). To characterize, by Fourier transform infrared (FTIR) spectroscopy, the biophysical changes in the SC lipids and proteins. (D). To study *in vitro* the macroscopic barrier changes in the skin by the above chemicals by measuring transepidermal water loss (TEWL). (E) To study the microscopic and ultramicroscopic alterations in skin due to JP-8 exposure. (F). To study the dermatotoxicity (skin barrier properties and irritation) of the above chemicals *in vivo* in rabbits. *In vitro* studies showed SC lipid and protein extraction, macroscopic barrier perturbation, and microscopic changes in JP-8 treated skin samples. Transmission electron micrograph showed many ultrastructural modifications in JP-8 treated porcine skin namely expansion in the intercellular spaces of the SC, reduction in compactness of tonofibrils of the SC, altered configuration and disrupted attachment of basale cells, reduction in dendritic processes of Langerhans' cells. In *in vitro* studies with JP-8 components, tridecane exhibited greater permeability through skin among aliphatic and naphthalene among aromatic JP-8 components, which may be due to their greater diffusion through skin. All of the chemicals caused significant ($p < 0.05$) increase in the *in vitro* TEWL values through skin. This indicates potential skin irritation and dermatotoxicity by JP-8 components. Amount of chemicals absorbed suggests that tridecane among aliphatic components and, naphthalene and its methyl derivatives among aromatic components should be monitored for their possible systemic toxicity. *In vivo* studies with JP-8 and its model components in rabbit showed an increase in temperature, capacitance, TEWL and severe to moderate erythema and edema with all test chemicals. The quantitative microscopic measurement results showed increase in epidermal thickness, and decrease in collagen fibers' bundle length and thickness. This constitutes potential dermatotoxicity from these chemicals. The DEPSCoR award provided research experience to a research associate, a graduate student and two professional (Pharm.D.) students and led to six publications in peer-reviewed journals and ten presentations in the national/international symposia and seminars.

Table of Contents

1. Objectives:

JP-8 is kerosene based multicomponent mixture of aromatic and aliphatic hydrocarbons, without the lower molecular weight fractions (Mattie et al., 1991). Hence, it is less volatile and has a higher flash point than JP-4. JP-8 has been associated with toxicity in animal models and humans (Grant et al., 2000, 2001; Harris et al., 2000; Riviere et al., 1999; Robledo et al., 1999; Rosenthal et al., 2001; Singh and Singh, 2001a; Ulrich, 1999; Ulrich and Lyons, 2000). There is a great potential for human exposure to JP-8. Although, inhalational exposure has been reduced due to its lower volatility than JP-4, there are situations when JP-8 gets aerosolized as aircraft engine starts at low ambient temperatures. These aerosols may be soaked to clothing, and thus may come into prolong contact with the skin of ground personnel. Splashes during refueling, handling of engine part coated with JP-8, contact with sides of fuel tanks during fuel maintenance operations, contact with fuel leaks on the undersides of aircraft or on ramp are potential sources of dermal exposure. Fuel system maintenance usually requires direct, prolonged exposure to fuel. Both military and commercial aircraft workers are at risk of dermal exposure and toxicity from JP-8 jet fuel. One of the most hazardous duties for USAF aircraft maintenance personnel is removal of foam from fuel tanks, as personnel receive dermal exposure to JP-8 jet fuel. Quantitation of penetration of chemicals through skin is necessary for assessment of health hazards involved in these occupational environments (McDougal et al., 1986; McDougal et al., 1990; EPA, 1989).

The skin serves as the primary interface between our internal and external environments. One of the main functions of the skin is as a barrier, but it is an incomplete barrier to some types of chemicals. As a result, there is potential for systemic toxicity from dermal absorption of chemicals if a large body surface area is to be exposed or the chemical penetrates the skin very well. There are needs for data and approaches to understand the human hazard from dermal exposure to JP-8.

We investigated the following **specific aims**:

(A). To determine percutaneous absorption of dodecane, tridecane, tetradecane, naphthalene, 1-methylnaphthalene, and 2-methylnaphthalene in vitro through dermatomed (0.5 mm thick) skin using Franz diffusion cells. The above chemicals are major components of JP-8 (present in JP-8 in a greater concentration than 1%).

(B). To study the binding of these chemicals to the stratum corneum (SC) by determining the partition coefficient in the SC/JP-8 system.

(C). To characterize, by Fourier transform infrared (FTIR) spectroscopy, the biophysical changes in the SC lipids of skin by the above chemicals. FTIR spectroscopy provides information on the vibrational modes of its components and probes the structure on a molecular level.

(D). To study *in vitro* the macroscopic barrier changes in the skin by the above chemicals by measuring transepidermal water loss (TEWL). TEWL provides a robust method for assessing macroscopic changes in the barrier properties of the skin.

(E) To study the microscopic and ultramicroscopic alterations in skin due to JP-8 exposure?

(F). To study the dermatotoxicity (skin barrier properties and irritation) of the above chemicals *in vivo* in rabbits by using the Draize visual scoring system, and to assess barrier function of the skin by measuring TEWL and skin capacitance. TEWL and skin capacitance provide an objective evaluation of changes in skin barrier function. Irritation tends to reduce the efficiency of the stratum corneum barrier function and results in a TEWL increase, which may be associated with a decrease in skin water content (skin capacitance).

2. EXPERIMENTAL METHODS

***In Vitro* Percutaneous Absorption:** Franz diffusion cells (Crown Bioscience, Inc., Clinton, NJ) were used in the *in vitro* percutaneous absorption studies. The skin was dermatomed to 0.5 mm thickness using Padgett Elecrtro Dermatome Instrument (Model B, Padgett Instrument Inc., Kansas city, MO, USA). The dermatomed skin was sandwiched between the cells with the epidermis facing the donor compartment. We have developed pig skin as a model for predicting percutaneous absorption of chemicals for humans. Therefore we have used pig skin in this study. The maximum capacities of the donor and receiver compartments were 1 and 5 ml, respectively, and the effective diffusion area was 0.785 cm^2. The donor compartment contained 1 ml of the radiolabelled test chemicals (4 μ Ci in 1 ml JP-8), and the receiver compartment was filled with 5 ml of phosphate buffered saline, pH 7.4 (PBS) containing 0.1 % formaldehyde and 0.2% Tween 80 to act as preservative and solubilizer, respectively. The cells were maintained at 37±0.5 °C by a PMC Dataplate® stirring digital dry block heater (Crown Bioscientific INC., Somerville, NJ). The content of the receiver compartment was stirred with a magnetic bar at 100 rpm. At appropriate times, 1 ml samples were withdrawn from the receiver compartment and

transferred to scintillation vials. After sampling, an equivalent amount of receiver fluid was added to the receiver compartment to maintain a constant volume.

The samples were assayed by liquid scintillation counting. Each sample was mixed with 10 ml of scintillation cocktail (Econosafe®, Research Products International Corp., Mount Prospect, IL) and was counted in a liquid scintillation counter (Packard, Tri Carb® 2100 TR, Downers Grove, IL) for quantification of ^{14}C in disintegration per minute (dpm). The instrument was programmed to give counts for 10 min. Net dpm for the samples were obtained by subtracting background dpm measured in the control samples. All experiments were performed in replicates of six, and the results were expressed as the mean ± SD of six experiments.

Binding of Chemicals to SC: The SC was prepared following the method of Kligman and Christophers (1963). The SC was pulverized in a mortar with a pestle and SC that passed through a 40–mesh sieve but was retained by a 60–mesh sieve was used. Ten milligram of pulverized SC was mixed by vortexing with 1 ml of JP-8 containing 4 μ Ci of the test chemical. The mixture was shaken for 10 h at 37 °C. After 10 h of contact time, the mixture was separated by centrifugation, and the supernatant was removed. The sediment was resuspended three times in JP-8 to remove chemical adsorbed on the surface (Wester et al., 1991). The amount of radioactivity in the supernatants was determined by liquid scintillation counting. The amount of chemical that bound to the SC was obtained by subtracting the amount of chemical recovered in supernatants from the amount of chemical originally added. Six sets of experiments were performed for each chemical.

Biophysical Properties of SC Lipids and Proteins by FTIR: The SC samples were treated for 24 h by applying 500 μl of chemical on 10 cm^2 area of SC in a closed petri dishes. The samples were vacuum-dried (650 mm Hg) at 21 ± 1°C for 3 days and stored in desiccator to evaporate JP-8 (Yamane et al., 1995). The treated SC was then subjected to FTIR spectroscopy. Spectra were obtained in the frequency range of 4000-1000 cm^{-1}. Attention was focused on characterizing the occurrence of peaks near 2850 and 2920 cm^{-1}, which were due to the symmetric and asymmetric C-H stretching, respectively. Strong amide absorbance occurred in the region of 1500-1700 cm^{-1} due to C=O stretching and N-H bending (Koenig and Snively, 1998). The decrease in peak

heights and areas of methylene and amide absorbances is related to the SC lipid and protein extraction, respectively (Bhatia and Singh, 1998; Bommannan et al., 1991; Goates and Knutson, 1994; Zhao and Singh, 2000). OMNIC® FTIR software (Nicolet Instrument Corporation, Madison, WI, USA) was used to calculate the peak heights and areas. For each SC sample, peak height and area were measured before and after the JP-8 treatment. This experimental strategy allowed each sample to serve as its own control.

Transepidermal Water Loss (TEWL) through Skin: Franz diffusion cells (Kai et al., 1993) were used for *in vitro* TEWL studies. The dermatomed skin was treated with chemical in a manner similar to the SC for FTIR. The treated dermatomed skin was then sandwiched between the diffusion cells with the SC side up and the dermal side exposed to the receiver compartment containing isotonic saline (0.9% sodium chloride solution). The surface area of the epidermis exposed for TEWL was 0.785 cm^2. The temperature of the diffusion cells was maintained at 37 ± 0.5°C. The dermatomed skin was allowed to equilibrate in the *in vitro* system for 4 h before TEWL measurements with Tewameter™ (Courage & Khazaka, Colgne and Acaderm, Menlo Park, CA, USA). TEWL measurements was performed by holding the Tewameter™ probe over the donor cell opening until a stable TEWL value was achieved. The experiments were performed in a room with an ambient temperature between 20°C to 26°C and relative humidity between 46% to 58%. In all the cases six replicates of experiments were performed, and the results expressed as the mean ± SD. Experiments were performed in the same manner without chemical treatment of the dermatomed skin to serve as control.

Light Microscopy of JP-8/Chemicals Exposed Skin: The dermatomed skin (0.5 mm thick, 10 mm x 5 mm size) was placed in a vial facing the dermal side towards the bottom of the vial. We added 0.5 ml JP-8 on the SC side of the skin and kept aside for 24 h. The treated and the control (untreated) samples were fixed in 10% neutrally buffered formalin solution (Accustain®). When required for use in light microscopy, these samples were washed with water for 7 h to remove excess fixative. Then, the samples were dehydrated by transferring successively to increasing strengths of alcohol, cleared by passing through toluene. Finally the samples were infiltrated and embedded in molten paraffin (Accumate™), cooled at room temperature and paraffin blocks were prepared. Sections of 10 μm were cut by rotatory microtome, mounted on a glass slide with

the help of glycerogelatin, stained with chrysoidine, hematoxylin and counter stained with eosin. At last, they were dehydrated, cleared, cover slipped, and examined under microscope (Humason, 1972; Luna, 1968). Microscopic structures observed were photographed by Polaroid® Microcam camera on 339 Polaroid Auto Films. Epidermal thickness, length and thickness of collagen fibers' bundle and follicular lumen thickness were measured quantitatively under a 100x lens (Meiji Microscope, Osaka, Japan) with the help of a Cole-Parmer Video Caliper (Model 49910-20, Cole-Parmer, Chicago, IL, USA).

For *in vivo* microscopic study, skin samples from different groups of rabbits were taken by punch biopsy immediately after patch removal and after 24 h of patch removal from the chemically treated and control sites. In each case, rabbits were euthanized before punch biopsy. We also took skin sample from the region where no patch was applied. These samples were fixed in 10% neutrally buffered formalin solution (Accustain®) and processed as discussed earlier.

Transmission Electron Microscopy of *in vitro* JP-8 Exposed Skin: The skin samples were treated with JP-8 for 24 hrs. The untreated skin sample was used as a control. The skin samples were then fixed in 2.5% gluteraldehyde in Millonig's phosphate buffer (pH 7.4). Post fixation was performed in 2% osmium tetroxide in Millonig's phosphate buffer (pH 7.4). The samples were dehydrated in graded acetone, stored in saturated uranyl acetate in 70% acetone, and embedded in Epon-araldite resin. Ultrathin transverse sections were cut on a ultramicrotome, stained with lead citrate, examined and photographed with a JEOL JEM 100 CX transmission electron microscope.

Skin Integrity and Irritation in Rabbits: Skin barrier function and primary irritation were measured *in vivo* in rabbits. The dorsal region of each rabbit was shaven carefully avoiding skin damages with the help of Oster Golden A5® single speed clipper using size 40 blade. Rabbit was acclimatized for 24 h before taking any measurements. Environmental conditions were monitored: room temperature 20-26^0 C, relative humidity 46-58%. TEWL was measured quantitatively with a Tewameter ™ (Courage & Khazaka, Cologne, FRG) using Fick's law of diffusion. The probe was held on the skin until a stable TEWL value established (1 min). The electrical capacitance (device internal unit, i.u.) of the skin surface was measured using

Corneometer™ SM 820 (Courage & Khazaka, Cologne, FRG). Skin temperature was measured using an infrared thermometer (Omega Engineering Inc., Stamford, CT). The visual scoring system was used to evaluate primary skin irritation manifested as erythema: very slight erythema barely perceptible # 1; well defined erythema # 2; moderate to severe erythema # 3; severe erythema, beet redness to slight eschar formation, injuries in depth # 4; and edema: very slight edema, barely perceptible # 1; slight edema, edges of area well defined by definite raising # 2; moderate edema, area raised approximately 1 mm # 3; severe edema, raised more than 1 mm, and extending beyond area of exposure # 4 (Draize et al., 1944).

Dorsal skin of each rabbit was marked into one cm^2 area at three places on the left side and three places on the right side. Each rabbit had three test sites and three control sites. Baseline measurements were taken corresponding to test and control sites. Haye's occlusive test chamber saturated with test chemical (50 µl) was placed at the test sites and chemical untreated chamber on the control sites; secured in place by pressing each chamber. After 24 h, patches were removed from both control and test sites. Skin measurements (e.g., transepidermal water loss, skin capacitance and visual Draize scores) were taken at 0 h, 1 h, 2 h, 4 h, and 24 h after removal of the patches. The primary planned comparisons involved the assessment of skin reactions to test chemicals in terms of measured responses. Response variables for the analysis were formed by subtracting the measurements recorded at the control site from that at the corresponding test site. This removed any occlusion effects, which may have been common to the test and control sites.

There was no need to anesthetize rabbits during experimentation because all procedures and measurements (TEWL, capacitance, and Draize visual scores) were non-invasive and painless. Rabbits were euthanized immediately after completion of the experiment by injecting pentobarbital sodium intravenously via ear vein at the dose of 100 mg/kg of body weight. All the experiments were performed in replicates of six.

Data Analysis: The chemical concentration was corrected for sampling effects using equation 1 (Hayton and Chen, 1982):

$$C'_n = C_n \left(V_T / V_T - V_S \right) \left(C'_{n-1} / C_{n-1} \right) \quad \text{.....(1)}$$

Where, C'_n is the corrected concentration of n^{th} sample, C_n the measured concentration of chemical in the n^{th} sample, C_{n-1} the measured concentration of the chemical in the $(n-1)^{th}$ sample, V_T the total volume of the receiver fluid, V_S the volume of the sample drawn.

The corrected chemical concentration was divided by the area of the skin exposed to the donor compartment to calculate the cumulative amount of chemical absorbed per unit area. The cumulative amount of the chemical absorbed per unit area is plotted against time and the slope of the linear portion of the plot gave steady state flux (J_{SS}).

The permeability coefficient (K_p) was calculated using equation 2 (Scheuplein, 1978):

$$K_p = J_{SS} / C_V \quad \text{..... (2)}$$

where, C_V is the total donor concentration.

The lag time (t_L) to reach steady state was determined from the x-intercept of the linear portion of the above plot.

The binding of chemicals to the SC (P) was calculated as (Zhao and Singh, 2000):

$$P = \frac{\text{Concentration of chemical in 1000 mg of powdered SC}}{\text{Concentration of chemical in 1000 mg JP-8}} \quad (3)$$

Diffusion coefficient, D, was calculated by using the following equation:

$$D = Kp \times h / P$$

where h was the thickness of the dermatomed skin (0.05 cm).

We predicted the total amount of each of the major components of JP-8 absorbed based upon their flux through the skin, total surface area exposed, and duration of exposure.

Amount of chemicals absorbed, W, in 8 h (assuming both hands, 0.25 m^2, exposed during foam removal in the fuel tank of jet engine) was calculated by

$$W \text{ (mg)} = \text{Corrected flux (mg/cm}^2\text{/h)} \times 8 \text{ h} \times 2500 \text{ cm}^2$$

$$\text{Corrected flux} = \text{Flux} \times (C_1/C_2)$$

where C_1 = Actual concentration of chemical in JP-8

C_2 = Concentration of Chemical in donor cell used in percutaneous absorption study

Statistical comparisons were made using the Student's t-test and analysis of variance (ANOVA). The level of significance was taken as $p<0.05$.

3. RESULTS

In vitro studies

FTIR spectroscopy: Fig. 1 shows FTIR spectrum of a typical SC in which strong methylene and amide absorbances have been obtained. Fig. 2 and Fig. 3 show FTIR spectra of control and 2, 4, 8, and 24 h JP-8 treated SC for lipid and protein absorbances, respectively. Tables 1 and 2 show percentage decrease in peak height and area in comparison to the control at all time points for asymmetric C-H and symmetric C-H absorbances, respectively. Tables 3 and 4 indicate percentage decease in peak height and area for C=O stretching and N-H bending vibrations, respectively. The results showed that the treatment of the SC with JP-8 to increasing exposure time led to correspondingly greater % decrease in the peak heights and areas of methylene and amide absorbances.

***In Vitro* Transepidermal Water Loss:** Fig.4 shows TEWL values through the control and JP-8 exposed skin. We found an increase in the TEWL values with increasing exposure times. TEWL was significantly higher ($p<0.05$) through 8 h and 24 h JP-8 exposed skin in comparison to control.

Light microscopy: Figs. 5 and 6 are the light micrographs of control and JP-8 treated skin, respectively. Fig. 6 shows swelling in the outermost epidermal layer. Quantitative microscopic measurements were carried out for epidermal, collagen bundles, and follicular lumen thickness at twenty-five randomly selected positions. Epidermal thickness was found to be 60.18 ± 16.41 μm ($n=25$) and 97.53 ± 15.71 μm ($n=25$) in control and in JP-8 treated skin, respectively. Thus, there was a significant ($p < 0.01$) increase in epidermal thickness in the JP-8 treated skin than the control. At higher magnification (X100) detachment of SC at some places was observed (Figs. 7 and 8).

In 24 h JP-8 treated porcine skin (Fig. 6), collagen fiber bundles were found comparatively shortened and thickened than the control skin (Fig. 5). Length of collagen fiber bundles was determined to be 66.67 ± 19.41 μm (n=25) and 41.33 ± 16.69 μm (n=25) in the control and treated porcine skin, respectively. Thus, the length of collagen fiber bundles was found to be significantly ($p < 0.01$) reduced in the treated porcine skin. Likewise, thickness of the collagen fibers bundles was determined to be 5.87 ± 1.81 μm (n=25) and 10.49 ± 2.61 μm (n=25) in the control and chemically treated skin, respectively. The thickness of collagen fiber bundles in treated skin was significantly ($p < 0.01$) increased. In control, the collagen fiber bundles appeared coarse and aggregated (Fig. 5). In treated skin, collagen fiber bundles were found shortened, less coarse, and rarefied (Fig. 6). In general, the dermal matrix was ruptured and inflamed in 24 h JP-8 treated skin. Thickness of follicle lumen was 16.52 ± 4.38 μm (n=25) and 41.5 ± 17.37 μm (n=25) in control and treated skin, respectively. Thus, we found a significant ($p<0.05$) increase in the thickness of follicle lumen in 24 h JP-8 treated skin.

Transmission Electron Microscopy: Figures 11a and 11b show the ultrastructure of control and treated porcine skin, respectively. Figure 7b shows that treatment with JP-8 has caused extensive disruption in the structural integrity of stratum corneum by expanding intercellular spaces and disintegrating the filamentous network of individual corneocytes. Large scale expansion in intercellular domains of SC is quite significant. Fig. 12a of treated skin reveals alteration in configuration of basale cells because they appear almost spherical while in untreated sample they are columnar (Fig. 11a). Moreover, the breakage of hemidesmosomes and desmosomes can be observed in Fig. 12b. In Fig. 12a the serrated keratinocytes are seen without any significant tonofilaments attached to them. There is significant reduction in the dendritic processes in treated sample (Fig.13b) in comparison to control sample (Fig. 13a).

Binding to SC: Table 5 shows that there is an increase in binding of both the aliphatic and aromatic JP-8 components to SC with increasing Log PC values. Bindings to SC are 8.76±0.74, 13.15±1.05, 15.85±1.36, 8.14±1.02, and 8.39±0.77 for DOD, TRI, TET, NAP, and 2-MN, respectively. Greater binding to SC was found with TET followed by TRI and others.

In vitro Percutaneous Absorption: Fig. 10 shows in vitro transport profile of chemicals through the skin from which we calculated the flux of chemicals. Table 6 shows the flux (Jss), permeability coefficient (Kp), diffusion coefficient (D), and lag time (Lag t) to reach steady state. TRI was found to exhibit greater Jss, Kp and D values followed by NAP, 2-NAP, DOD, and TET. Jss depends on concentration of permeant in donor solution. 4 μCi of each chemical was used in 1ml of donor solution, which were equivalent to 519.48 nmol/ml, 74.76 nmol/ml, 221 nmol/ml, 493.83 nmol/ml, and 470.58 nmol/ml of DOD, TRI, TET, NAP, and 2-MN, respectively. Permeability coefficient is independent of concentration of permeant in the donor solution. TRI exhibited higher permeability coefficient (Kp) value, which was also bound to SC more.

Table 6 shows the diffusion coefficient values of five chemicals, which are $(0.21\pm0.02) \times 10^{-6}$ cm^2/h, $(6.84\pm0.57) \times 10^{-6}$ cm^2/h, $(0.20\pm0.04) \times 10^{-6}$ cm^2/h, $(1.30\pm0.27) \times 10^{-6}$ cm^2/h, and $(0.69\pm0.16) \times 10^{-6}$ cm^2/h, for DOD, TRI, TET, NAP, and 2-MN, respectively. Lag time is the time required by the permeant molecule to reach a steady state flux. A lower lag time indicates higher permeability coefficient. Table 6 indicate lower lag time for TRI among aliphatic and for NAP among aromatic components of JP-8, which are also transported more among their respective category.

FTIR spectroscopy: FTIR results in tables 3-6 suggest that all of the chemicals significantly ($p<0.05$) extracted SC lipid and protein in comparison to control. TRI extracted lipid and protein more than DOD, NAP, or 2-MN, hence also transported more than that of these chemicals. There was no significant ($p<0.05$) difference among NAP and 2-MN with respect to their SC lipid and protein extraction.

TEWL through the Skin: Table 11 shows the TEWL values of control and chemically treated porcine skin. All of the test chemicals caused significant ($p<0.05$) increase in TEWL in comparison to control. For TRI an increase in TEWL value was found maximum (29.22 ± 0.99 $g/m^2/h$) followed by NAP (25.08 ± 0.55 $g/m^2/h$), DOD (15.15 ± 1.34 $g/m^2/h$), 2-MN (14.76 ± 0.42 $g/m^2/h$), and TET (11.64 ± 1.42 $g/m^2/h$).

Body Burden of JP-8 Components: Table 12 shows the amount of chemicals absorbed assuming both hands (0.25 m^2 surface area) exposed for 8 h. Among five major components of JP-8 studied, TRI was found maximally absorbed (1624.81±124.10 mg) followed by NAP (48.38±6.31 mg), 2-MN (48.38±6.31 mg), TET (38.33±4.39 mg), and DOD (35.10±2.02 mg).

***In vivo* in rabbit JP-8/components exposure to skin**

Skin Integrity and Irritation: Fig. 16 shows the changes in temperature at different time points (0 h, 1 h, 2 h, 4 h, and 24 h) after removal of patches in comparison to temperature at the same site before application of patches. We found significant ($p<0.05$) increase in temperature at chemically treated sites immediately (0 h) after removal of patches in comparison to temperature before application of patches. Greater increase ($p<0.05$) in temperature was observed at TRI treated site at all time points followed by NAP, 1-MN, and 2-MN. However, we did not observe an increase in the temperature ($p>0.05$) at 4 h or 24 h of patch removal than before application of the patches in case of NAP, 1-MN, and 2-MN. At control site, temperatures at different time points after removal of patch were not significantly ($p<0.05$) different.

Fig. 17 shows the change in capacitance at different time points after removal of patches in comparison to capacitance at the same site before application of the patches. TRI caused greater increase in capacitance than other chemicals, however, the increase was not significant ($p>0.05$) except at 0 h, in comparison to the control at the same time point. There was an increase in the skin capacitance immediately after removal of the patches in all cases followed by gradual decrease at later time points.

Fig. 18 shows changes in the TEWL values at different time points (0 h, 1 h, 2 h, 4 h, and 24 h) after removal of patches in comparison to TEWL at the same site before application of patches. There was no significant ($p>0.05$) increase in TEWL at control sites at all time points. All the chemicals caused an increase in TEWL at all time points after removal of the patches in comparison to TEWL before application of the patches. TRI caused greater increase in TEWL followed by NAP, 1-MN, 2-MN, TET, and DOD. Increase in TEWL by TRI was significant ($p<0.05$) at all time points in comparison to increase in TEWL at control sites.

Table 13 and table 14 shows Draize scores for erythema and edema, respectively, at different time points after removal of chemical containing patches. All of the chemicals and JP-8 itself caused moderate to severe erythema and edema, which were not resolved to the baseline level even after 24 h of patch removal.

Light Microscopy: Fig. 19 shows epidermal thickness (ET), collagen fibers' bundle length (CL), and collagen fibers' bundle thickness (CT) at 0 h and 24 h of patch removal. We did not find any significant ($p<0.05$) difference in ET, CL, and CT between the skin samples from the site without patch and with control patch (Fig. 20a and b). All chemically treated sites significantly ($p<0.05$) increased ET in comparison to the control (patch without chemical) (Fig. 21a and b). We found significant ($p<0.05$) decrease in CL in skin samples taken from sites immediately (0 h) after removal of chemically treated patches in comparison to the control, which were not found to regain the original length in samples taken 24 h after patch removal except in case of TET. TRI decreased CL greater ($p<0.05$) than others (Fig. 22a, b, c and d). Likewise, all the chemicals decreased CT significantly ($p<0.05$) in comparison to the control in both 0 h and 24 h skin samples except 24 h TET treated skin.

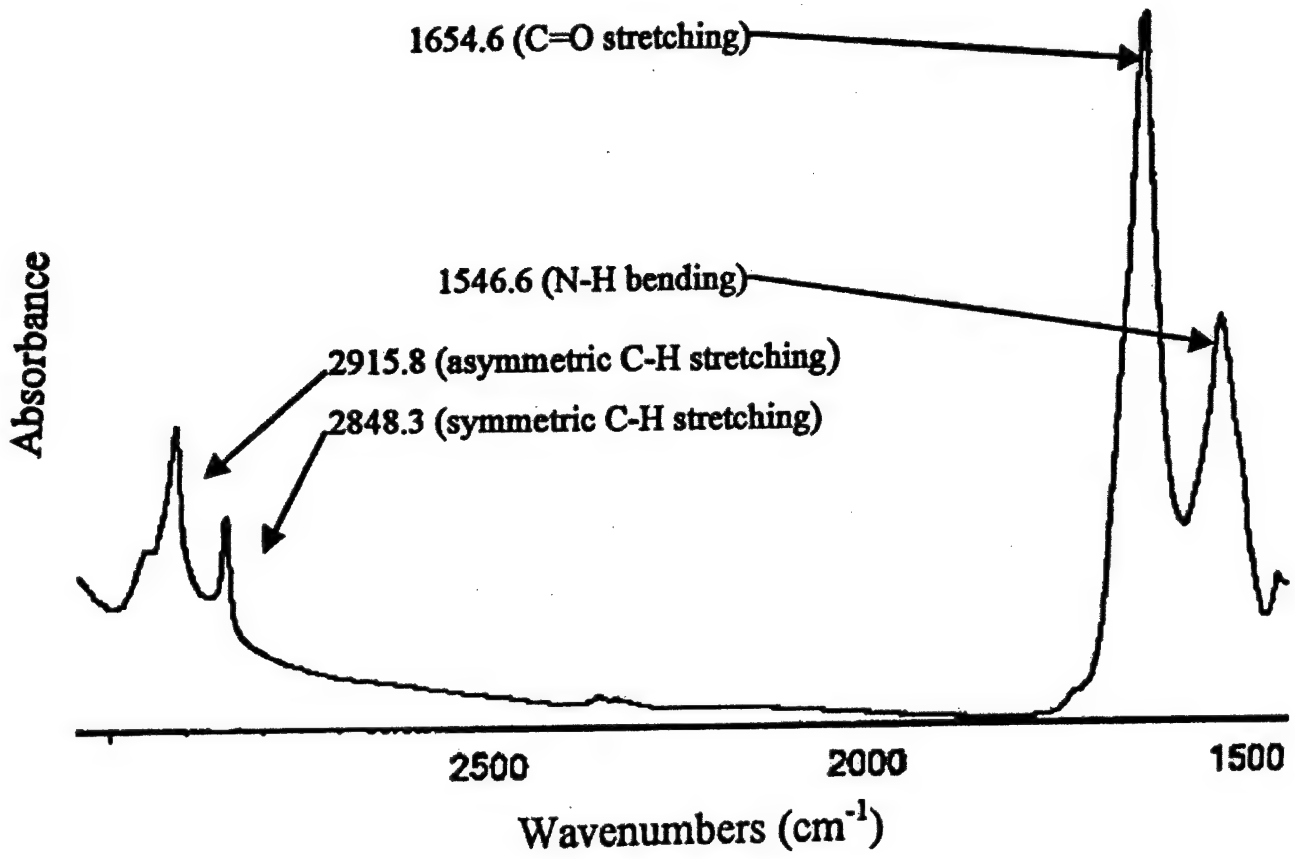

Figure 1. Fourier transform infrared spectroscopy (FTIR) spectrum of stratum corneum. Asymmetric and symmetric C-H stretching absorbances are due to lipid bilayer and C=O stretching and N-H bending absorbances are due to intercellular protein.

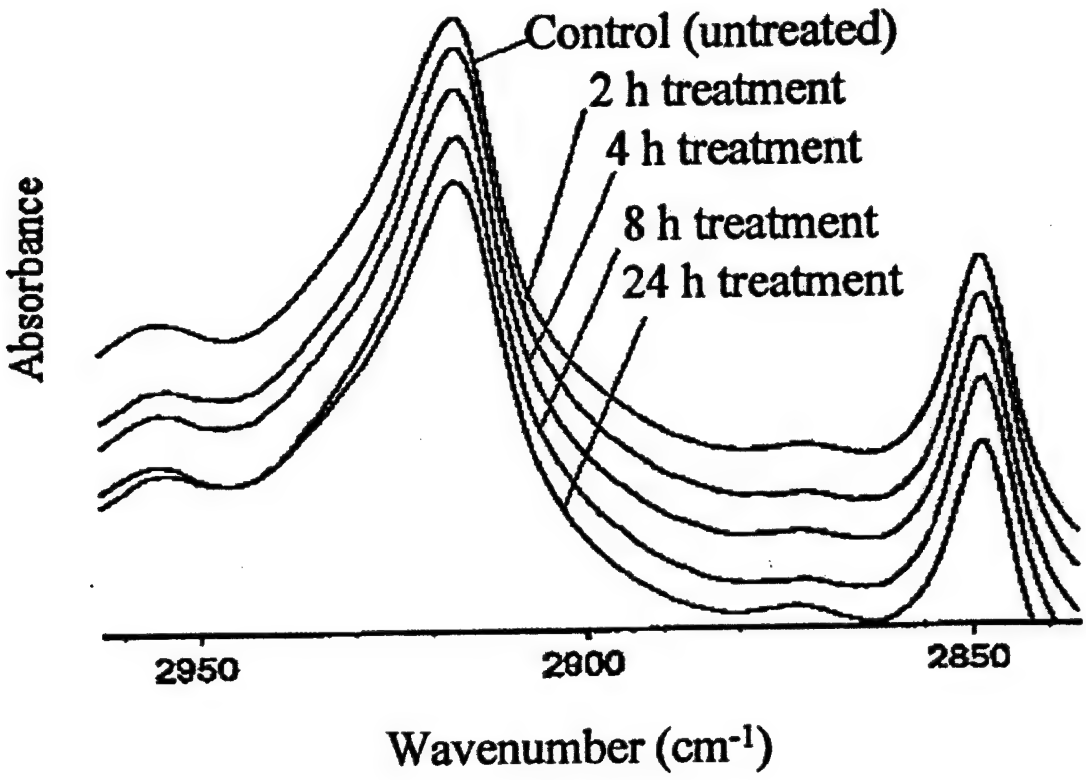

Figure 2. Effect of jet propellant-8 fuel on the peak height and area of asymmetric and symmetric C-H absorbances indicating extraction of lipid from stratum corneum.

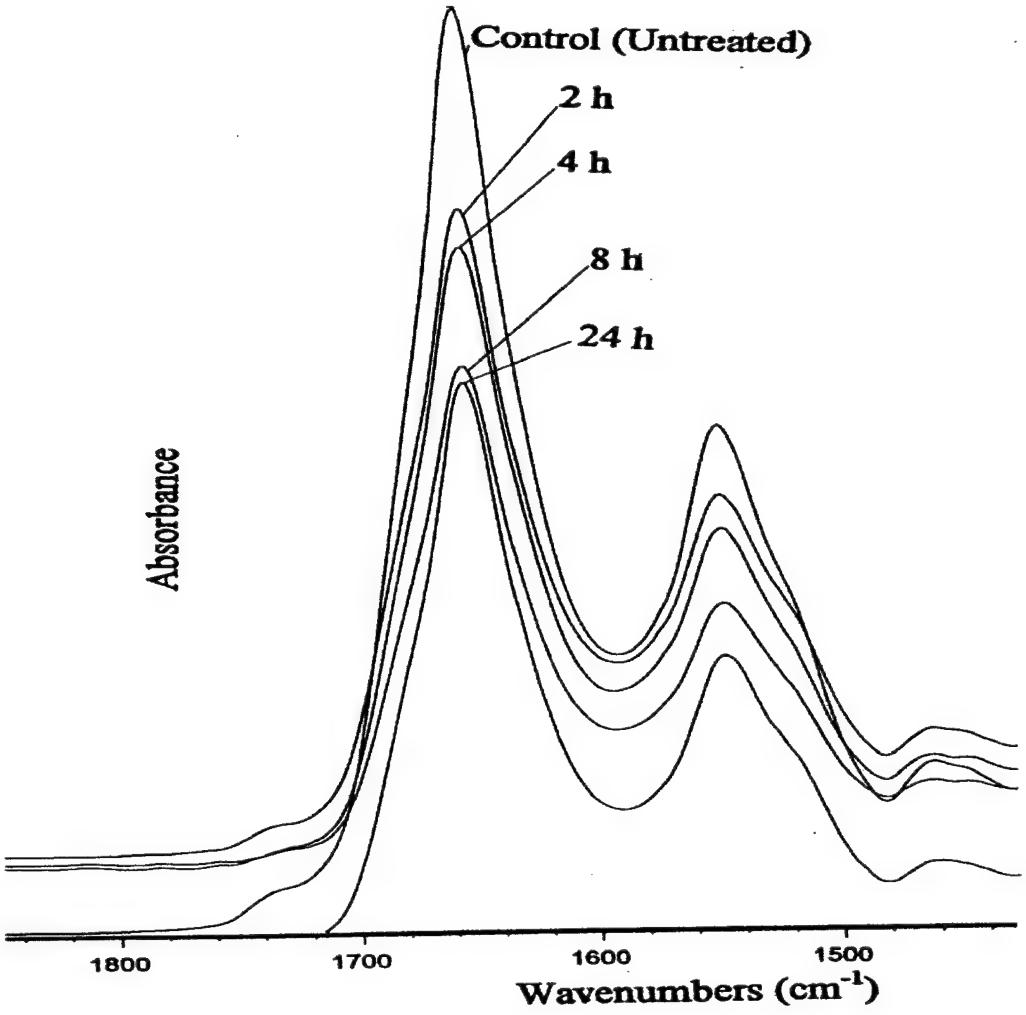

Figure 3. Effect of jet propellant-8 fuel jet fuel on the peak height and areas of C=O stretching and N-H bending absorbances indicating extraction of protein from stratum corneum.

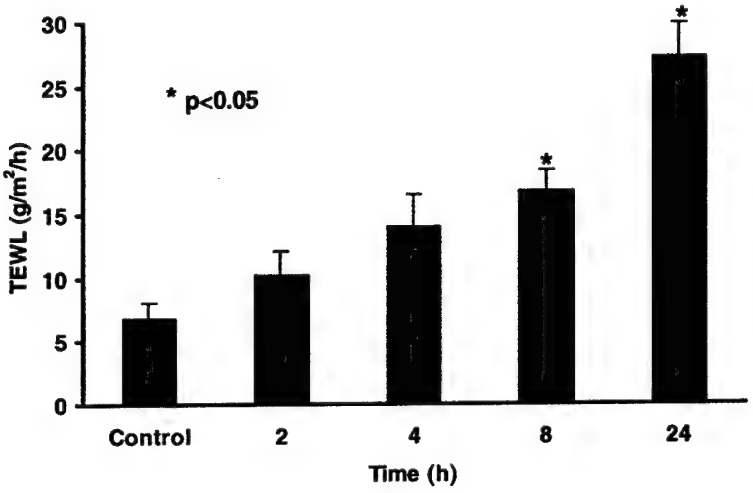

Figure 4. Effect of jet propellant-8 fuel on Transepidermal Water Losss(TEWL) through the skin. Increase in TEWL measurements at 8 h and 24 h were significantly ($p<0.05$) different from the control.

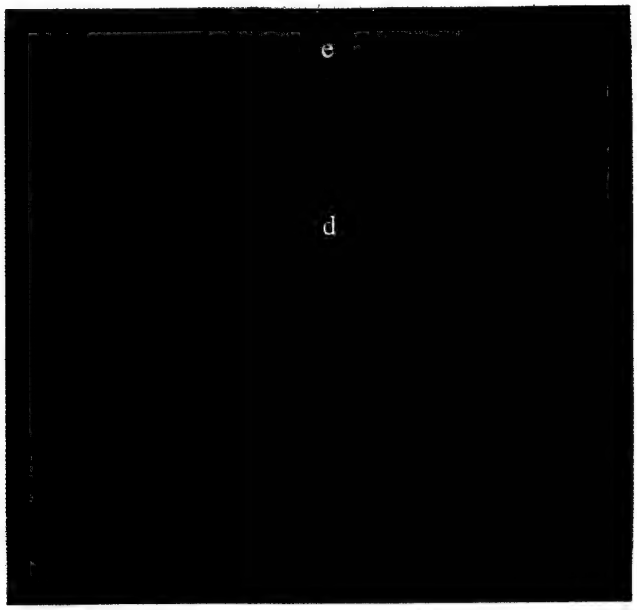

Figure 5. Light micrograph of control (untreated) skin. Normalepidermis (e) and dermis (d) are apparent, magnification X40.

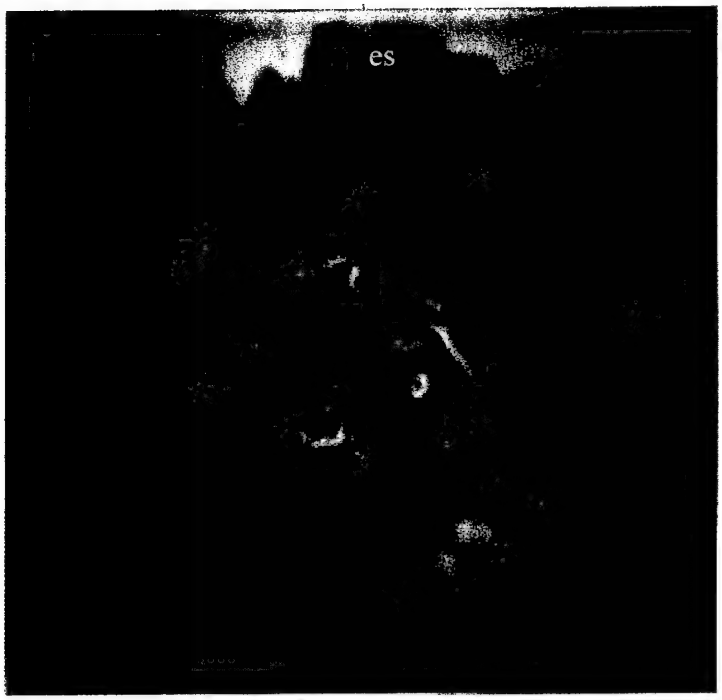

Figure 6. Light micrograph of jet propellant-8 treated (24 h) skin. Epidermal swelling (es) and dermal inflammation/rupture are visible, magnification X40.

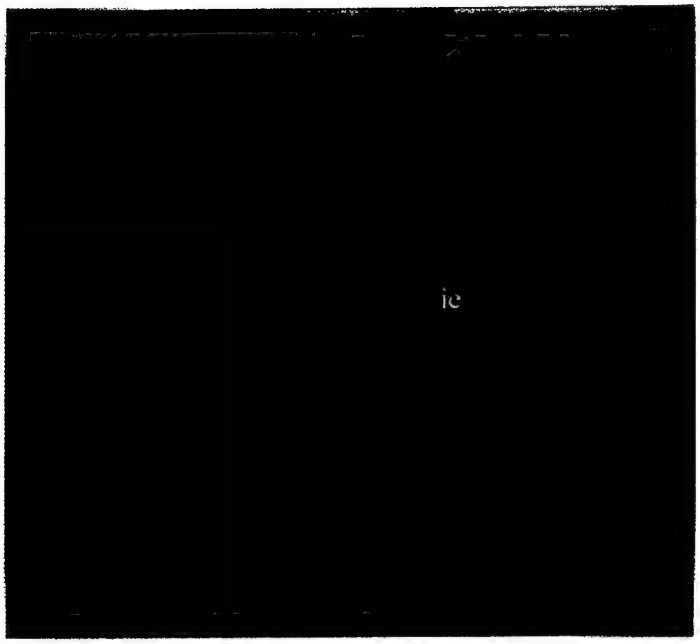

Figure 7. Light micrograph of control (untreated) skin. Epidermal (ie) layer without any rupture or detachment is noted, magnification X100.

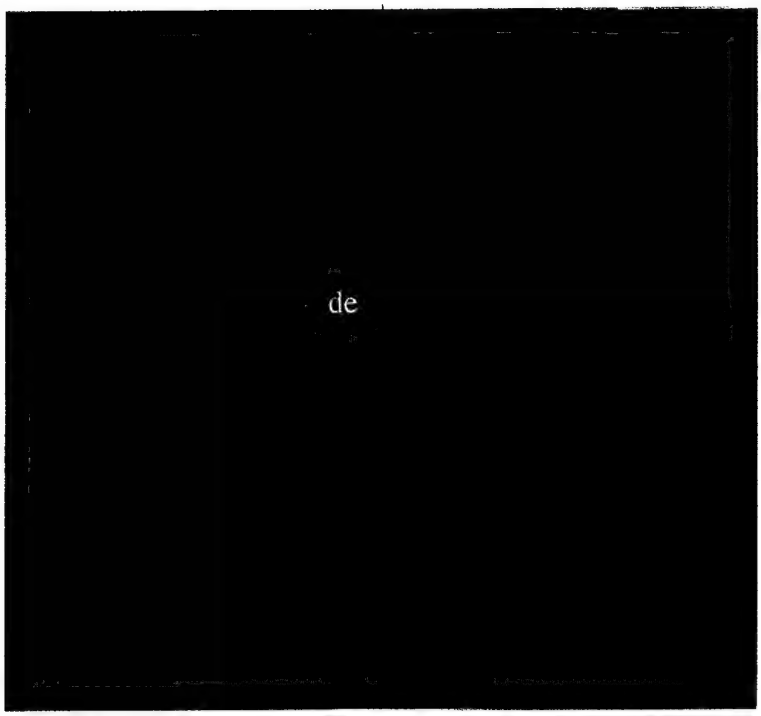

Figure 8. Light micrograph of jet propellant-8 treated (24 h) skin. Rupture and detachment (de) are quite obvious in epidermal region, magnification X100.

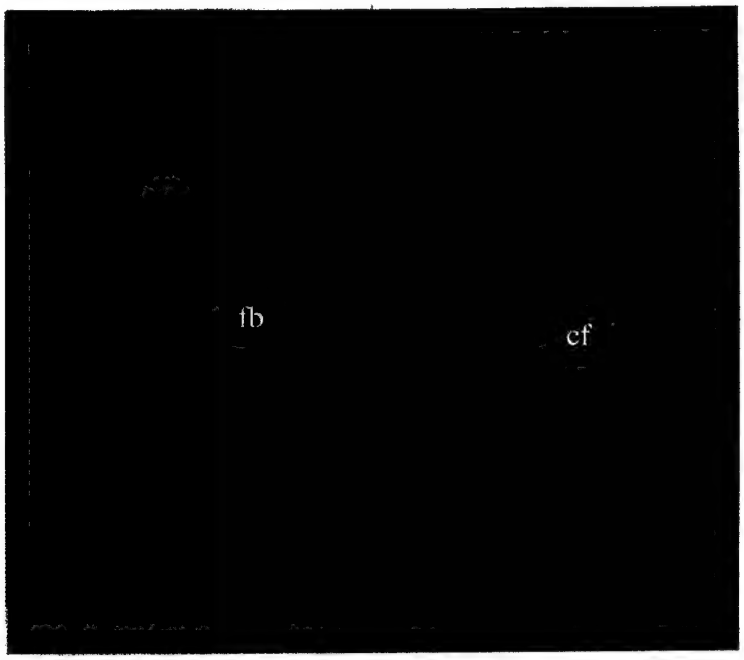

Figure 9. Light micrograph of control (untreated) skin. Collagen fibers' bundle (cf) and few fibroblasts can be seen, magnification X100.

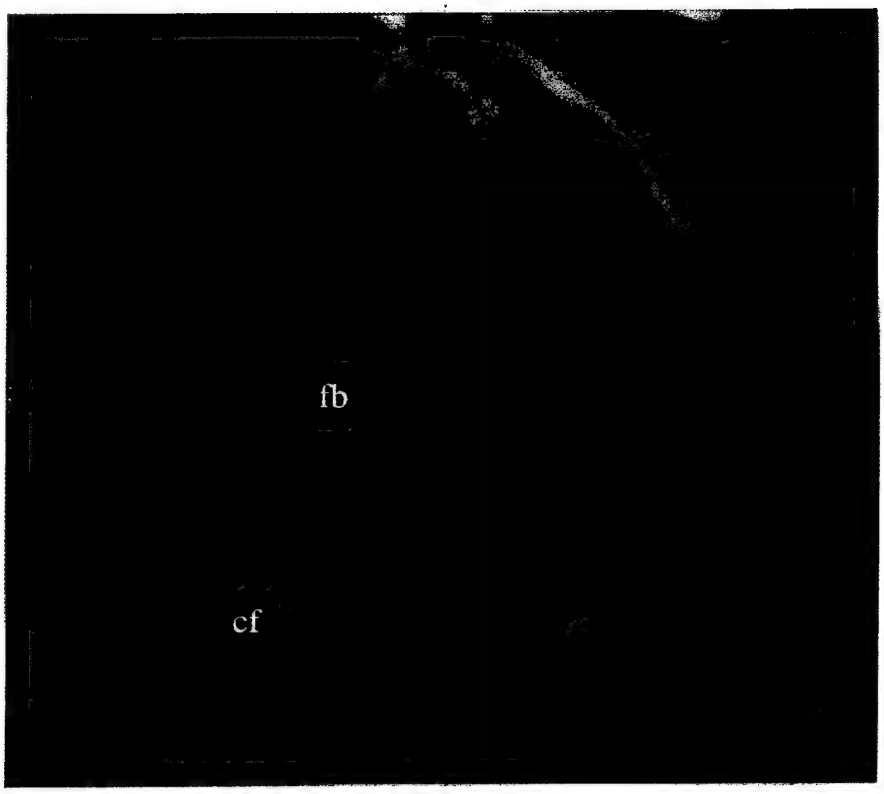

Figure 10. Light micrograph of jet propellant-8 fuel treated (24 h) skin. Shortening of collagen fibers' bundle (cf), greater number of fibroblast (fb), and dermal inflammation are notable, magnification X100.

Figure 11a. Transmission electron micrograph of control (C) skin. The micrograph shows stratum corneum (SC) and columnar basal cells (SB).

Figure 11b. Transmission electron micrograph of JP-8 treated (T) skin. An extensive disruption in stratum corneum (SC) is noted.

Figure 12a. Transmission electron micrograph of JP-8 treated (T) skin showing distortion in basal cell configuration (sb), less coarse prickle cell tonofibrils (tf), and serrated keratinocytes (k) without tonofilaments.

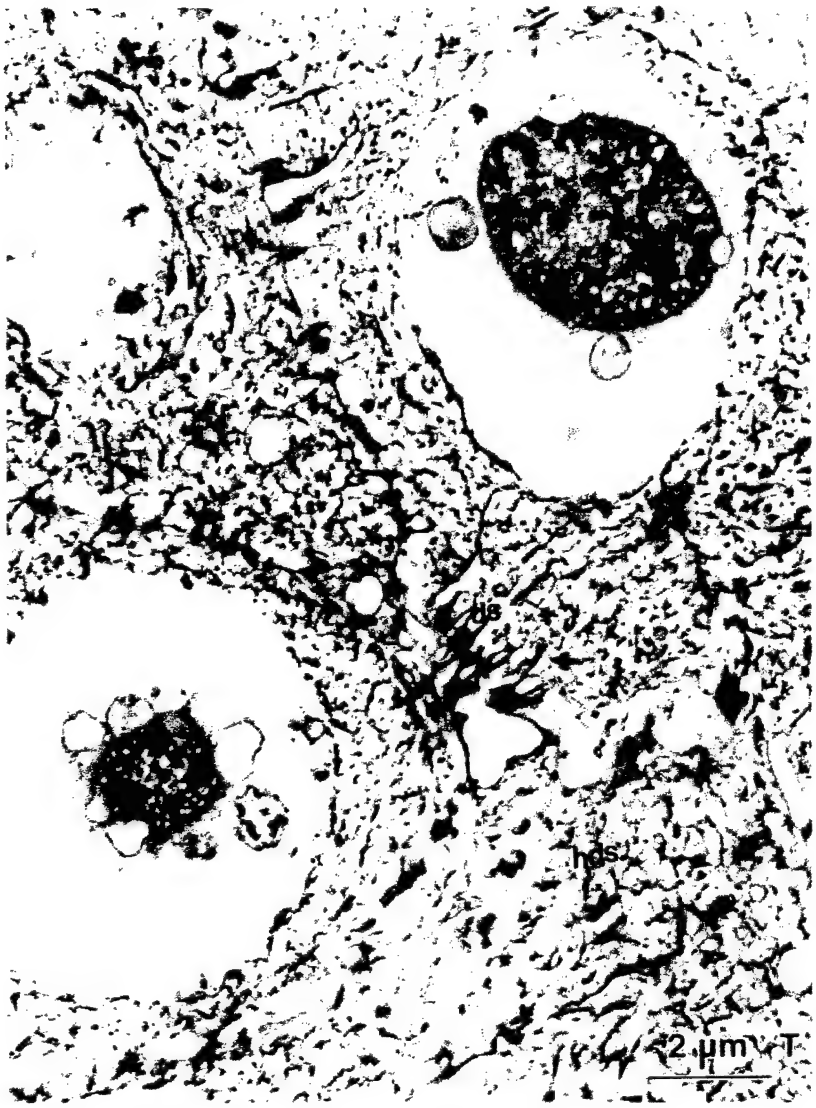

Figure 12b. Transmission electron micrograph of JP-8 treated (T) skin. Breaking of desmosomes (ds) and hemidesmosomes (hds) are noted in the micrograph.

Figure 13a. Transmission electron micrograph of control (C) skin showing well developed dendritic process (dp).

Figure 13b. Transmission electron micrograph of JP-8 treated (T) skin showing diminished dendritic process (ddp) in Langerhans cell of skin.

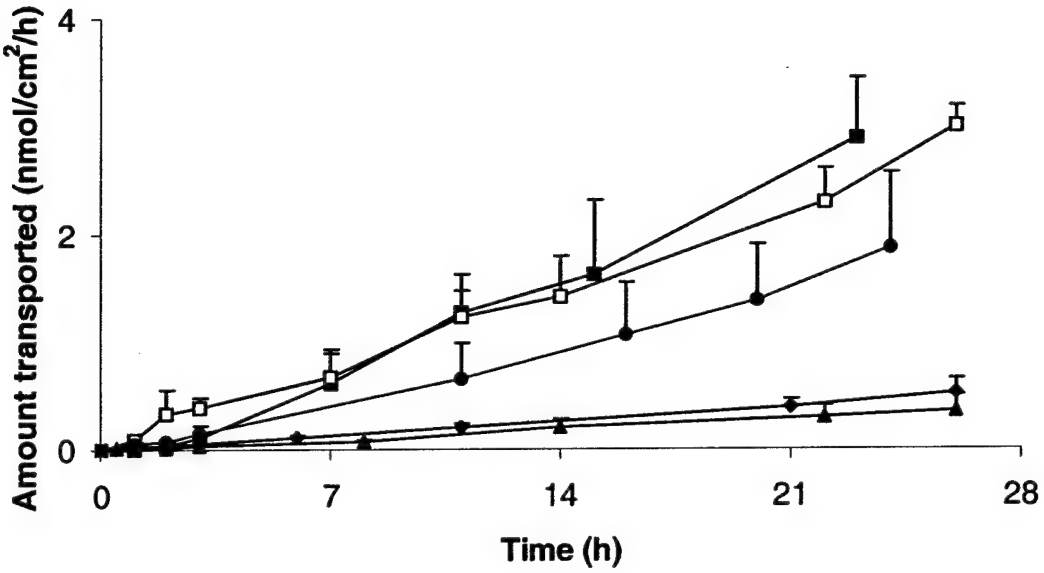

Figure 14. Transport of chemicals through dermatomed skin.

Key: (◆) Dodecane; (■) Tridecane; (▲) Tetradecane; ( ) Naphthalene;

(•) 2-Methylnaphthalene

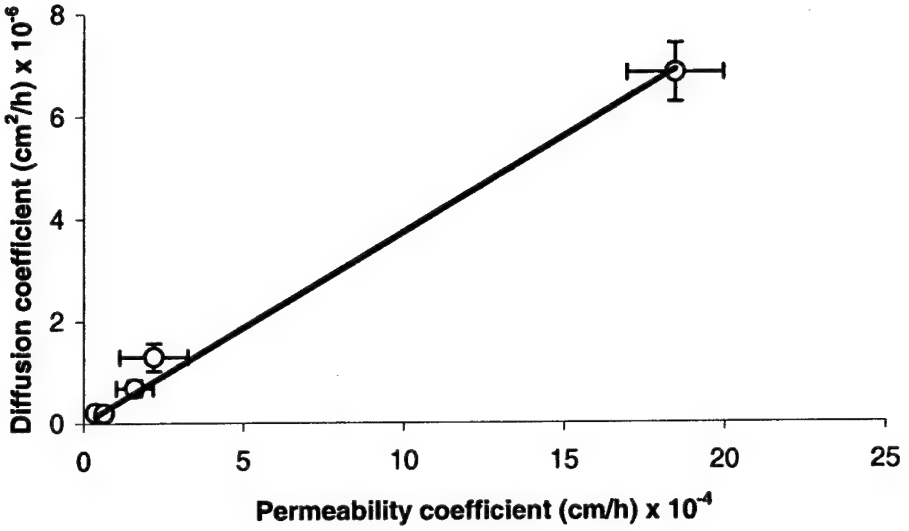

Figure 15. Correlation between permeability and diffusion coefficients of aliphatic and aromatic constituents of JP-8 jet fuel.

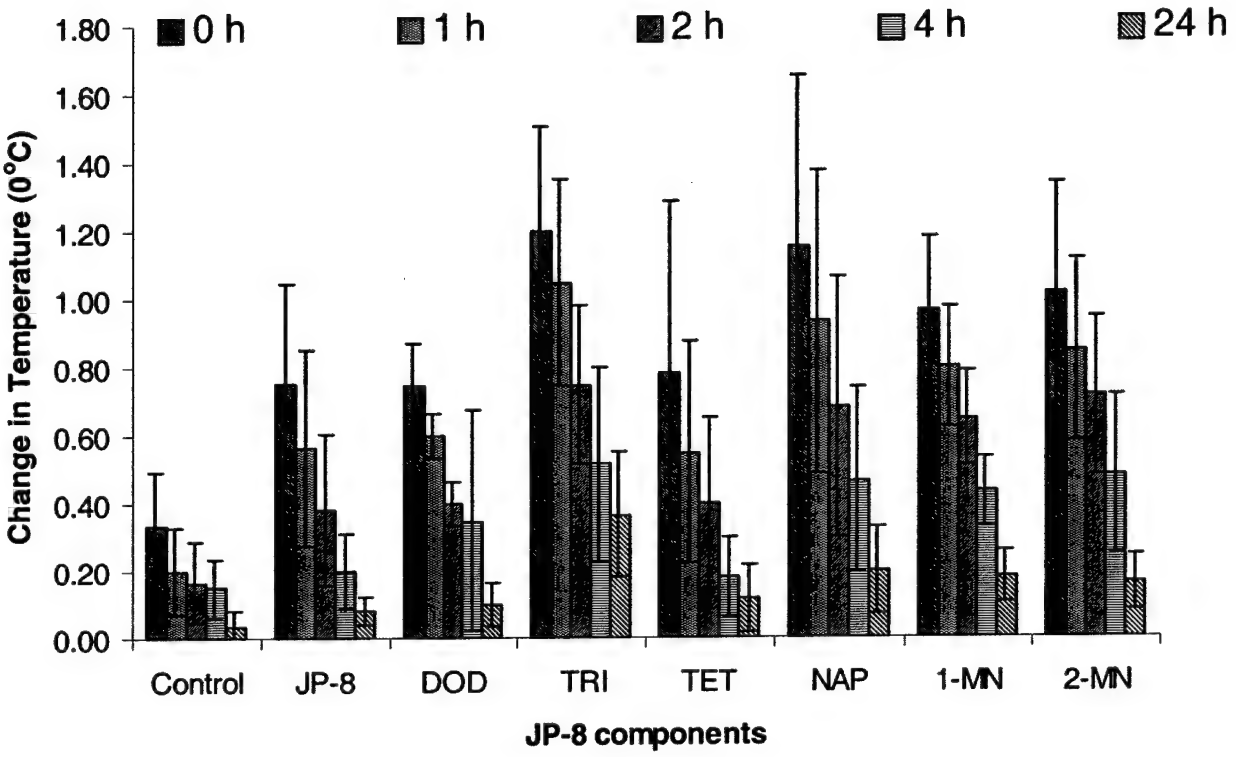

Figure 16. Changes in the temperature at 0 h, 1 h, 2 h, 4 h, and 24 h after patch removal in comparison to temperature at the same site before application of patch. All data are mean±S.D., n=6.

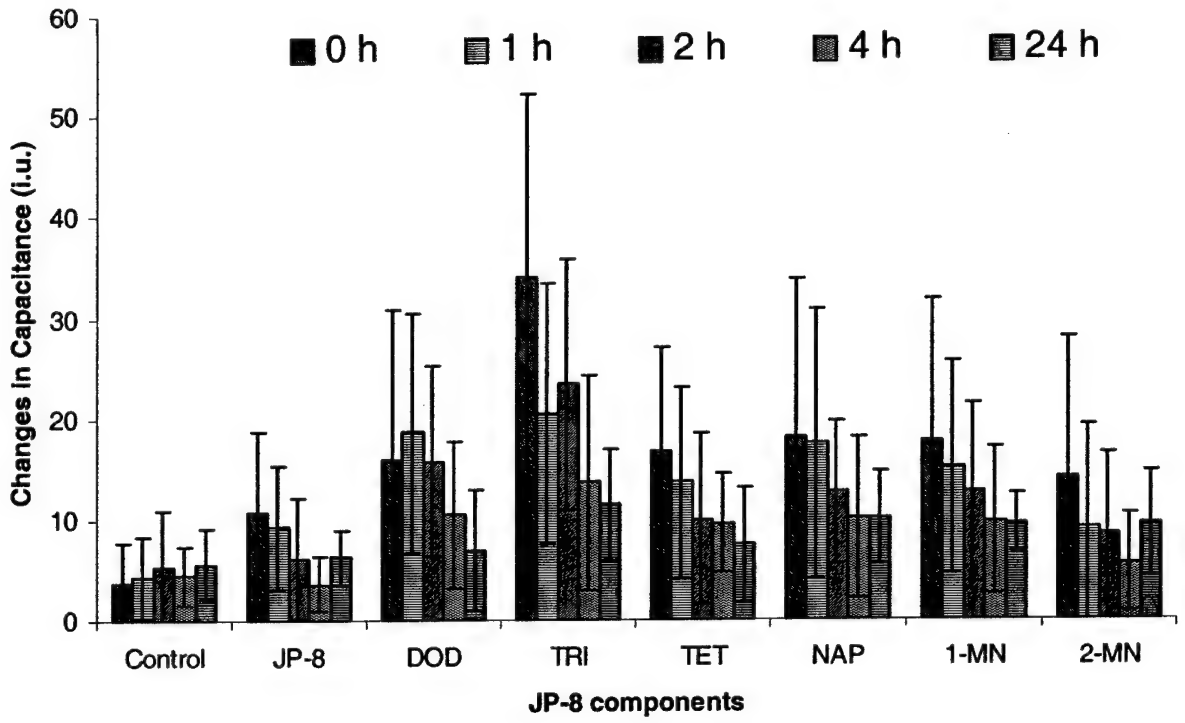

Figure 17. Changes in the capacitance at 0 h, 1 h, 2 h, 4 h, and 24 h after patch removal in comparison to temperature at the same site before application of patch. . All data are mean±S.D., n=6.

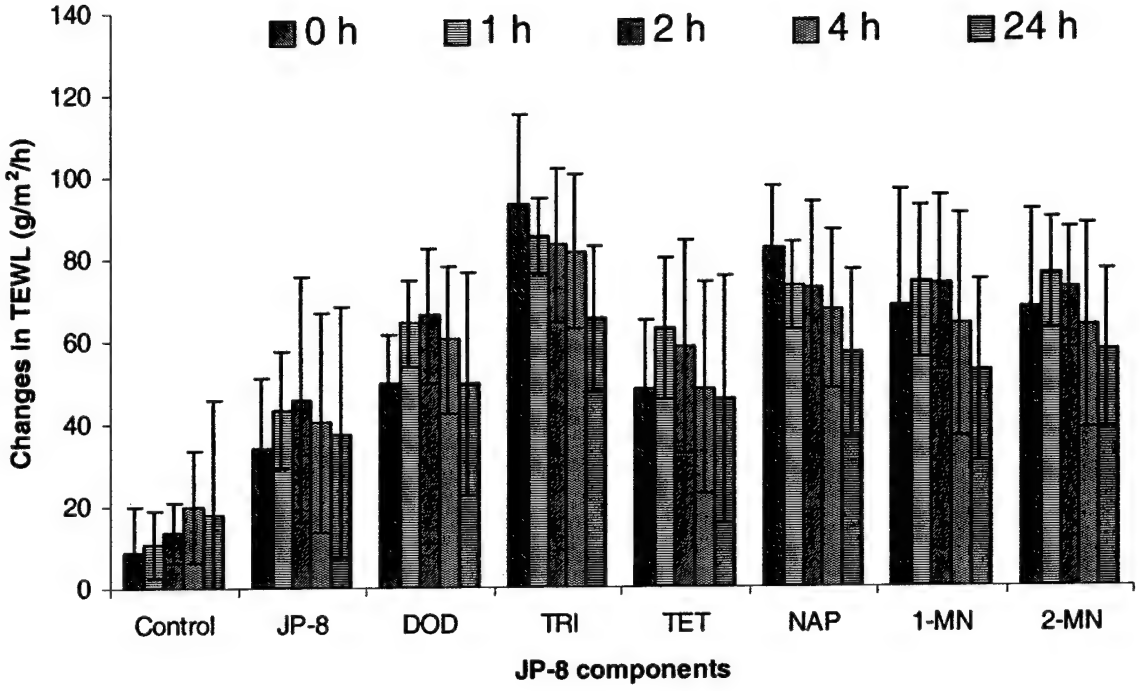

Figure 18. Changes in the TEWL at 0 h, 1 h, 2 h, 4 h, and 24 h after patch removal in comparison to temperature at the same site before application of patch. All data are mean±S.D., n=6.

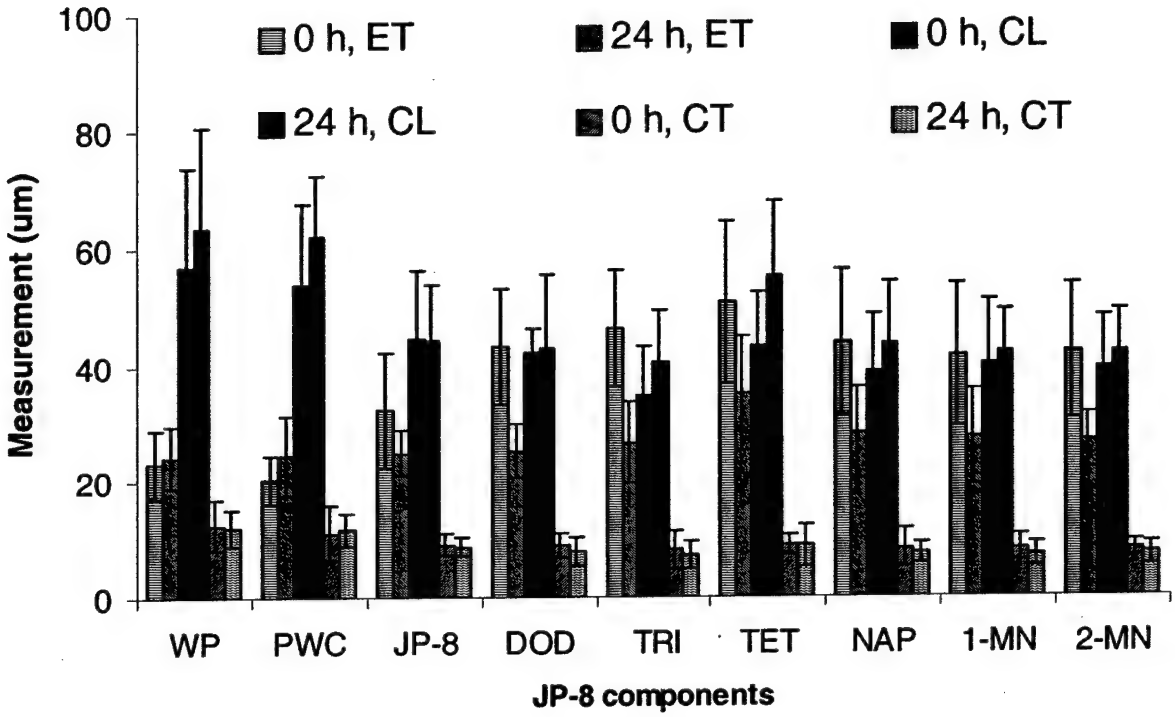

Figure 19. Epidermal thickness (ET), collagen fibers' bundle length (CL), and collagen fibers' bundle thickness at 0 h, and 24 h after patch removal. (Key: WP = Without patch no chemical, PWC = Control with patch but no chemical, JP-8 = Jet fuel propellent-8, DOD = Dodecane, TRI = Tridecane, TET = Tetradecane, NAP = Napthalene, 1-MN = 1-Methylnaphthalene, 2-MN = 2-Methylnaphthalene). . All data are mean±S.D., n=30.

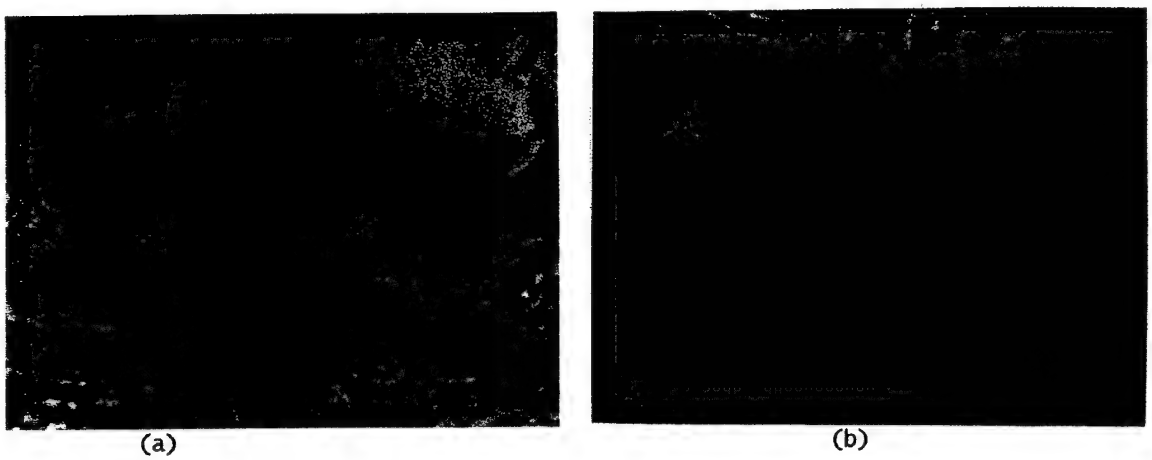

Figure 20. Light micrographs of control (patch without JP-8 components) skin samples (a) Control at 24 h, (b) Control at 0 h (E = Epidermis, CFB = Collagen fibers' bundle) X 40.

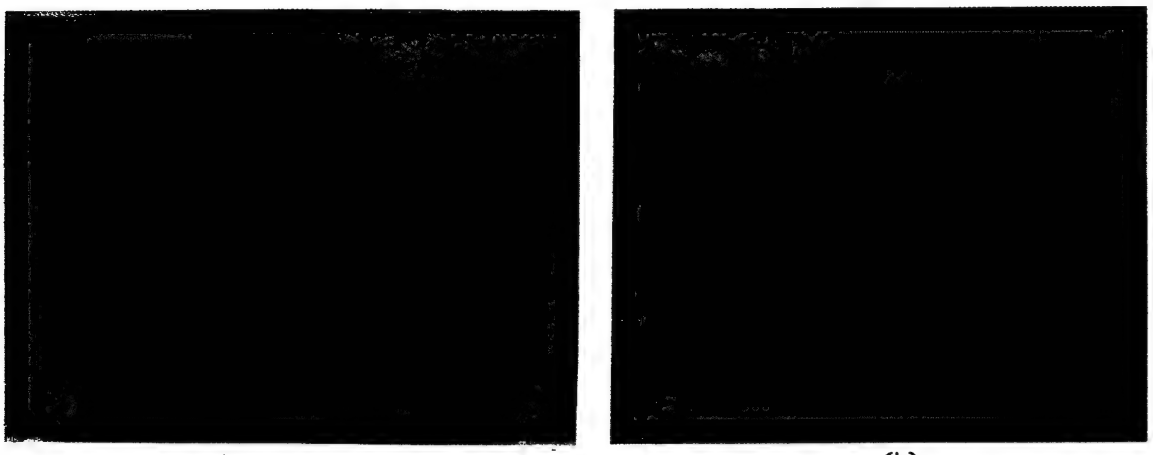

(a) (b)

Figure 21. (a) Light micrograph of skin sample after 24 h of patch removal containing tridecane, (b) Light micrograph of skin sample after 0 h of patch removal containing tridecane (E = Epidermis, CFB = Collagen fibers' bundle, FB = Fibroblast) X 40.

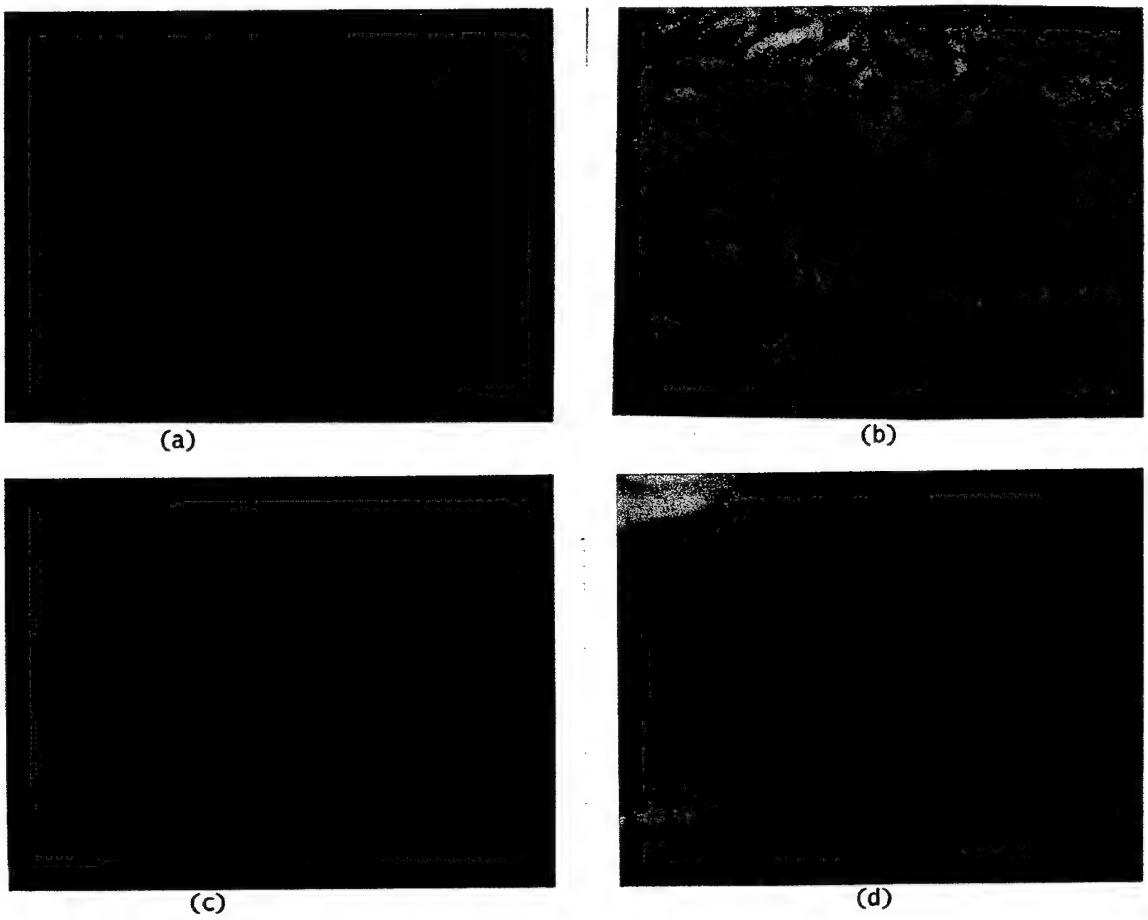

Figure 22. Light micrograph of skin sample showing changes in collagen fibers' bundles (a) Control at 0 h, (b) 0 h after removing tridecane containing patch (c) 24 h after removing tridecane containing patch, (d) 24 after removing tetradecane containing patch ((E = Epidermis, CFB = Collagen fibers' bundle, FB = Fibroblast, V = Extensive disruption) X 40.

Table 1. Percentage decrease in the peak height and peak area of asymmetric C-H stretching absorbance of jet propellant-8 fuel treated stratum corneum

	Asymmetric C-H stretching					
	Peak height (Mean ± SD, n=6)			Peak area (Mean ± SD, n=6)		
Treatment	Control	Treated	% Decrease[a]	Control	Treated	% Decrease[a]
2 h	1.18 ± 0.21	1.04 ± 0.19	12.08 ± 0.92	19.53 ± 3.05	16.89 ± 2.61	13.53 ± 0.93
4 h	1.19 ± 0.08	1.01 ± 0.05	15.04 ± 1.20	20.46 ± 0.76	16.92 ± 0.70	17.30 ± 1.59
8 h	1.07 ± 0.19	0.85 ± 0.15	19.53 ± 1.10	19.11 ± 2.06	14.84 ± 1.62	22.36 ± 1.79
24 h	1.33 ± 0.23	1.03 ± 0.17	22.63 ± 0.89	20.72 ± 3.00	16.07 ± 2.38	22.44 ± 1.12

[a] % Decrease in peak height or area was calculated from the following equation:

$$\%\ \text{Decrease in peak height or area} = \frac{(\text{Peak height or area from control}) - (\text{Peak height or area from treated})}{\text{Peak height or area from control}} \times 100$$

Table 2. Percentage decrease in the peak height and peak area of symmetric C-H stretchingabsorbance of the jet propellant-8 fuel treated stratum corneum

	Symmetric C-H stretching					
	Peak height (Mean±SD, n = 6)			Peak area (Mean±SD, n = 6)		
Treatment	Control	Treated	% Decrease[a]	Control	Treated	% Decrease[a]
2 h	0.63±0.11	0.55±0.10	13.05±1.10	8.72±1.60	7.60±1.40	12.87±1.22
4 h	0.63±0.08	0.53±0.06	16.51±1.10	8.95±0.53	7.58±0.52	15.34±0.09
8 h	0.64±0.04	0.49±0.03	23.44±1.04	8.97±0.52	7.26±0.41	19.13±1.00
24 h	0.73±0.15	0.57±0.12	22.47±0.71	8.21±1.45	6.29±1.07	23.25±1.16

[a] % Decrease in peak height or area was calculated from the following equation:

$$\%\ \text{Decrease in peak height or area} = \frac{(\text{Peak height or area from control}) - (\text{Peak height or area from treated})}{\text{Peak height or area from control}} \times 100$$

Table 3. Percentage decrease in the peak height and peak area of C=O stretching absorbance of the jet propellant-8 fuel treated stratum corneum

	C=O stretching					
	Peak height (Mean±SD, n = 6)			Peak area (Mean±SD, n = 6)		
Treatment	Control	Treated	% Decrease[a]	Control	Treated	% Decrease[a]
2 h	2.36±0.32	2.09±0.29	11.60±0.47	100.90±13.87	88.72±12.53	12.10±0.91
4 h	2.37±0.27	2.03±0.24	14.47±0.90	106.34±8.79	90.76±7.70	14.67±0.45
8 h	2.44±0.15	2.02±0.14	17.17±0.63	108.54±6.14	89.76±4.65	17.28±0.52
24 h	2.52±0.75	1.96±0.57	22.32±1.13	120.91±15.80	92.91±9.63	23.08±1.20

[a] % Decrease in peak height or area was calculated from the following equation:

$$\%\ \text{Decrease in peak height or area} = \frac{(\text{Peak height or area from control}) - (\text{Peak height or area from treated})}{\text{Peak height or area from control}} \times 100$$

Table 4. Percentage decrease in the peak height and peak area of N-H bending absorbance of the jet propellant-8 fuel treated stratum corneum

	N-H bending					
	Peak height (Mean±SD, n = 6)			Peak area (Mean±SD, n = 6)		
Treatment	Control	Treated	% Decrease[a]	Control	Treated	% Decrease[a]
2 h	1.06±0.12	0.92±0.19	13.20±0.89	38.36±3.30	33.51±2.75	12.62±0.80
4 h	1.12±0.10	0.95±0.09	15.01±0.62	40.25±2.06	34.00±1.71	15.51±0.58
8 h	1.18±0.09	0.95±0.06	18.83±1.45	40.13±3.04	32.77±2.51	18.35±1.06
24 h	1.36±0.33	1.04±0.26	23.41±0.84	41.01±9.63	31.89±7.75	22.38±1.01

[a] % Decrease in peak height or area was calculated from the following equation:

$$\% \text{ Decrease in peak height or area} = \frac{(\text{Peak height or area from control}) - (\text{Peak height or area from treated})}{\text{Peak height or area from control}} \times 100$$

Table 5. Log P and binding of chemicals to SC

Chemicals	Log PC	Binding to SC (P) (Mean±SD, n = 6)
Dodecane	6.10	8.76±0.74
Tridecane	6.73	13.15±1.05
Tetradecane	7.20	15.85±1.36
Naphthalene	3.30	8.14±1.02
2-Methylnaphthalene	3.86	8.39± 0.77

Log PC (Octanol/ Water) was estimated using C log P software.

Table 6. Percutaneous absorption parameters of five chemicals*

Chemicals	Jss (nmol/cm^2/h) x 10^{-2}	Kp (cm/h) x 10^{-4}	D (cm^2/h) x 10^{-6}	Lag t (h)
Dodecane	1.94±0.39	0.37±0.13	0.21±0.02	1.33±0.07
Tridecane	13.80±0.82	18.46±1.50	6.84±0.57	0.89±0.17
Tetradecane	1.40±0.20	0.64±0.20	0.20±0.04	1.62±0.34
Naphthalene	10.87± 1.47	2.20±1.07	1.30±0.27	1.19±0.01
2-MN	7.59±1.07	1.60±0.58	0.69±0.16	1.36±0.04

Jss = Steady state flux; Kp = Permeability coefficient; D = Diffusion coefficient; Lag t = Lag time to reach steady state transport of chemicals.

* All data are (Mean ± SD, n = 6).

Table 7. Percent decrease in the peak height and peak area of asymmetric C-H stretching absorbance of the SC*

	Asymmetric C-H stretching					
	Peak height			Peak area		
Chemicals	Control	Treated	% Decrease [a]	Control	Treated	% Decrease [a]
Dodecane	3.88±0.29	2.93±0.12	24.29±3.62	28.28±2.02	21.50±2.05	24.07±2.58
Tridecane	3.68±0.31	2.54±0.29	31.15±0.45	27.89±2.53	20.32±1.08	26.89±3.90
Tetradecane	3.46±0.41	2.18±0.43	37.59±7.12	28.89±2.59	20.56±2.72	29.11±4.33
Naphthalene	3.79±0.48	3.12±0.47	17.93±2.84	27.86±2.34	22.57±2.33	19.11±2.22
2-Methyl naphthalene	3.53±0.77	2.79±0.39	19.54±9.19	27.73±1.75	22.76±2.61	18.19±6.00

[a] % Decrease in peak height or area was calculated from the following equation:

$$\%\ \text{Decrease in peak height or area} = \frac{(\text{Peak height or area from control}) - (\text{Peak height or area from treated})}{(\text{Peak height or area from control})} \times 100$$

* All data are (Mean ± SD, n = 6).

Table 8. Percent decrease in the peak height and peak area of symmetric C-H stretching absorbance of the SC*

	Symmetric C-H stretching					
	Peak height			Peak area		
Chemicals	Control	Treated	% Decrease [a]	Control	Treated	% Decrease [a]
Dodecane	2.51±0.02	1.92±0.19	23.62±2.09	14.21±0.62	10.74±1.07	24.60±5.99
Tridecane	2.45±0.25	1.79±0.08	26.50±5.99	13.35±0.42	9.97±0.76	25.42±4.73
Tetradecane	2.26±0.19	1.51±0.22	33.53±5.86	13.89±0.31	8.91±0.72	35.94±5.30
Naphthalene	2.24±0.17	1.80±0.19	19.82±3.39	14.24±0.38	11.57±0.73	18.82±4.18
2-Methyl naphthalene	2.51±0.16	2.05±0.18	18.45±2.79	13.69±0.25	10.96±0.46	19.97±2.68

[a] % Decrease in peak height or area was calculated from the following equation:

$$\%\ \text{Decrease in peak height or area} = \frac{(\text{Peak height or area from control}) - (\text{Peak height or area from treated})}{(\text{Peak height or area from control})} \times 100$$

*All data are (Mean ± SD, n = 6).

Table 9. Percent decrease in the peak height and peak area of C=O stretching absorbance of the SC*

	C=O stretching					
	Peak height			Peak area		
Chemicals	Control	Treated	% Decrease [a]	Control	Treated	% Decrease [a]
Dodecane	5.56±1.43	4.13±0.76	24.22±8.23	259.89±13.82	195.96±24.49	24.88±7.68
Tridecane	6.56±1.13	4.63±0.41	28.37±8.61	276.84±15.52	194.27±17.17	29.95±3.22
Tetradecane	5.38±0.95	3.26±0.24	38.27±9.10	246.64±11.55	149.34±15.32	39.61±4.78
Naphthalene	5.67±0.85	4.59±0.73	19.16±1.06	241.48±4.58	197.45±10.27	18.19±0.97
2-Methyl naphthalene	5.78±0.63	4.65±0.68	19.88±4.29	231.42±14.82	186.23±21.92	19.80±6.13

[a] % Decrease in peak height or area was calculated from the following equation:

$$\%\ \text{Decrease in peak height or area} = \frac{(\text{Peak height or area from control}) - (\text{Peak height or area from treated})}{(\text{Peak height or area from control})} \times 100$$

*All data are (Mean ± SD, n = 6).

Table 10. Percent decrease in the peak height and peak area of N-H bending absorbance of the porcine SC*

	N-H bending					
	Peak height			Peak area		
Chemicals	Control	Treated	% Decrease [a]	Control	Treated	% Decrease [a]
Dodecane	3.35±0.27	2.53±0.26	24.61±2.38	97.83±7.37	72.83±2.05	25.29±4.99
Tridecane	3.25±0.24	2.24±0.25	31.27±3.70	107.83±7.47	75.62±1.08	29.60±5.48
Tetradecane	3.15±0.21	1.89±0.23	40.22±4.69	101.53±6.98	60.12±2.72	40.69±1.98
Naphthalene	3.45±0.29	2.85±0.31	17.56±2.90	91.27±4.56	73.63±2.35	19.25±2.09
2-Methyl naphthalene	3.05±0.23	2.42±0.15	20.57±1.51	87.59±2.85	69.84±2.61	20.28±0.55

[a] % Decrease in peak height or area was calculated from the following equation:

$$\%\ \text{Decrease in peak height or area} = \frac{(\text{Peak height or area from control}) - (\text{Peak height or area from treated})}{(\text{Peak height or area from control})} \times 100$$

***All data are (Mean ± SD, n = 6).**

Table 11. *In vitro* transepidermal water loss (TEWL) through chemically treated skin

Chemicals	TEWL (g/m^2 h, mean ± S.D, n = 6)	
	Control skin	Treated skin
Dodecane	9.71±0.88	24.86±2.22 ($p<0.05$)
Tridecane	8.87±1.01	38.93±1.89 ($p<0.05$)
Tetradecane	8.90±0.93	19.10±0.95 ($p<0.05$)
Naphthalene	8.44±1.42	33.95±0.46 ($p<0.05$)
2-Methyl naphthalene	8.91±0.65	23.67±0.23 ($p<0.05$)

Student's t-test was used to find the difference in TEWL of treated group from the control.

Table 12. Predicted amount of aliphatic and aromatic components of JP-8 absorbed through the exposed skin (0.25 cm^2) during 8 h exposure period

Chemical	Amount absorbed (mg) (Mean ± S.D, n = 6)
Dodecane	35.10±2.02
Tridecane	1624.81±124.10
Tetradecane	38.33±4.39
Naphthalene	48.42±5.84
2-Methylnaphthalene	48.38±6.31

Table 13. *In vivo* in rabbit erythema scores at different time points after removal of patches

	Draize score for erythema (Mean±SD, n=6)					
Chemicals	Before	0 h	1 h	2 h	4 h	24 h
Control	0±0.00	0±0.00	0±0.00	0±0.00	0±0.00	0±0.00
JP-8	0±0.00	1±0.41	1±0.41	1±0.41	1±0.52	2±0.82
DOD	0±0.00	1±0.52	1±0.52	1±0.41	1±0.00	1±0.41
TRI	0±0.00	2±0.82	2±0.52	2±0.55	2±0.55	2±0.75
TET	0±0.00	1±0.52	1±0.75	1±0.89	1±0.89	1±0.84
NAP	0±0.00	2±0.52	2±0.52	2±0.84	1±0.75	2±0.82
1-MN	0±0.00	2±0.41	2±0.41	2±0.41	1±0.52	1±0.52
2-MN	0±0.00	2±0.41	2±0.41	2±0.41	1±0.52	2±0.89

Control = Patch without chemical

DOD = Dodecane, TRI = Tridecane, TET = Tetradecane, NAP = Naphthalene, 1-MN = 1-methylnaphthalene, 2-MN = 2-methylnaphthalene

Table 14. *In vivo* in rabbit edema scores at different time points after removal of patches

	Draize score for edema (Mean±SD, n=6)					
Chemicals	Before	0 h	1 h	2 h	4 h	24 h
Control	0±0.00	0±0.00	0±0.00	0±0.00	0±0.00	0±0.00
JP-8	0±0.00	2±0.52	2±0.11	1±0.52	2±0.41	2±0.98
DOD	0±0.00	2±0.98	2±0.88	1±0.52	2±0.84	1±1.10
TRI	0±0.00	2±0.75	2±0.87	2±0.75	2±0.89	2±1.03
TET	0±0.00	2±0.55	2±0.71	1±0.41	1±0.52	1±0.41
NAP	0±0.00	2±0.82	2±1.03	2±0.89	2±0.98	2±1.05
1-MN	0±0.00	2±0.52	2±0.79	2±0.52	1±0.52	1±0.75
2-MN	0±0.00	2±0.89	2±0.95	2±0.89	2±0.89	2±0.98

Control = Patch without chemical

DOD = Dodecane, TRI = Tridecane, TET = Tetradecane, NAP = Naphthalene, 1-MN = 1-methylnaphthalene, 2-MN = 2-methylnaphthalene

3. DISCUSSION:

The FTIR results suggest that the treatment of the SC with JP-8 for 24 h causes lipid and protein extraction from SC. Since lipid plays an important role in SC barrier functions (Scheuplein & Blank, 1971), lipid extraction signifies disruption of barrier function of SC and its comparatively greater vulnerability than that of control to environmental toxicants or chemical toxicity brought about by JP-8 exposure.

The keratin filaments of SC contain proteins – loricrin and profilaggrin (Steven et el., 1990). The cross-linked protein complex of corneocytes envelope is insoluble and chemically resistant. These proteins play an important role in the structural assembly of the intercellular lipid lamellae of the SC (Lazo et al., 1995). Therefore, protein extraction from the SC due to JP-8 treatment suggests disturbances in the epidermal permeability barrier along with obstruction in epidermal flexibility and differentiation, which may be implicated in various dermatological disorders.

Irritation tends to reduce the efficiency of the SC barrier function and results in an increase in TEWL. Fig.4 indicates that JP-8 exposure for 8 and 24 h produced significant ($p<0.05$) increase in TEWL in comparison to the control. TEWL measurements are regarded as an indicator of barrier function; a high TEWL generally indicates barrier perturbation. Several investigators (Elias, 1983; Wertz and Downing, 1982) have suggested that the high resistance of the SC to water flux is due to the extended multilamellar lipid domains present intercellularly in the SC. Accordingly, molecules must traverse the hydrocarbon regions of these lamellae in order to diffuse across this barrier. It is generally accepted that a solvent, such as ethanol, removes intercellular material, which results in cutaneous barrier disruption (Scheuplein and Blank, 1971). Hence, an increased TEWL through the skin after 8 and 24 hours of JP-8 exposure is due to the corresponding increase in the lipid extraction by JP-8, as evident by FTIR findings. Light microscopy further provided visual evidences of the microscopic changes in the skin caused by JP-8 exposure. We observed significant increase in epidermal thickness and detachment of SC at some places, which indicates perturbation of SC barrier properties. The dermis, a critical organ of the body, not only provides the nutritive, immune, and other support systems for the epidermis through a thin papillary layer adjacent to the epidermis but also plays a

role in temperature, pressure, and pain regulation. The dermis consists of collagenous fibers (70%), and elastic connective tissue, in a semigel matrix of mucopolysaccharides (Roberts and Walters, 1998). In 24 h JP-8 treated porcine skin (Fig. 6), collagen fibers' bundles were found comparatively shortened and thickened than that in the control skin (Fig. 5). The thickness of collagen fibers' bundle in treated skin was significantly ($p < 0.01$) increased. In control, the collagen fibers were bundled together and hence, appeared coarse and aggregated (Fig. 5). In treated skin, collagen fibers' bundles were found shortened less coarse and rarefied (Fig. 6). In general, whole of the dermal matrix is seen rarefied and swelled in 24 h JP-8 treated skin. These changes in collagen fibers' bundle are indicative of dermal absorption of JP-8, which may lead to disruption of nutrient supply to epidermal layer.

The main cells present in the dermis are fibroblasts, which produce the connective tissue components of collagen, laminin, fibronectin and vitronectin; mast cells, which are involved in the immune and inflammatory responses; and melanocytes, involved in the production of the pigment melanin (Roberts & Walters, 1998). Fig. 9 showed fewer fibroblasts in control porcine skin. However, fig.10 showed a greater number of fibroblasts in JP-8 treated porcine skin than the control, which suggest some kinds of immune reaction and inflammatory processes caused by JP-8 (Ulrich, 1999; Ulrich and Lyons, 2000; Singh and Singh, 2001a). The outermost layer of epidermis, stratum corneum, is a unique structural composite forming the ultimate barrier between life and the surrounding environment. This is consisted of cornified, flattened, keratnized cells without nuclei and cytoplasmic organelles. These keratinized cells are surrounded by a three dimensional, multilamellar lipid domain (Monteiro-Riviere, 1991). Large scale expansion and disruption in intercellular domains of stratum corneum is quite significant (Fig. 11b). Large vacuolization indicate entry of JP-8 into the corneocyte cytosol and disruption of keratin.

Alteration in configuration of basal cells (Fig. 12a) and breakage of hemidesmosomes and desmosomes (Fig. 12b) are in fact very much noteworthy modifications. This is the stratum basale layer, consisted of a single layer of columnar or cuboidal shaped cells (Breathnach, 1971; Monteiro-Riviere and Stromberg, 1985) joined together laterally and to the overlying stratum spinosum cells by desmosomes, and to the irregular shaped basement membrane by

hemidesmosomes, which makes contact with an extracellular membrane (Elias, 1989), called basement membrane. This is the junction between epidermis and dermis, and is essential for the survival of the epidermal cells, because they get nutrients from dermis through it. Hence the alteration in configuration and disruption in contact mechanism will certainly impair the nutrient supply from dermis to cells of viable layer (epidermis).

There are two morphologically distinct types of basale keratinocytes: the nonserrated cells and the serrated cells. The serrated cells are relatively large and columnar in shape, and are characterized ultrastructurally by numerous bundles of tonofilaments, which extend all the way to the tips of the cytoplasmic projections. The nonserrated cells are smaller, cuboidal and have a paucity of tonofilaments (Lavker and Sun, 1982). The serrated cells are thought to anchor the epidermis (Lavker and Sun, 1983). Appearance of the serrated keratinocytes without any significant tonofilaments (Fig. 12a) may lead to interference with the synthesis of keratin. Absence of dark keratinocytes (Fig 12a) may indicate that JP-8 exposure is not causing generation of tumors because dark basale keratinocytes (Klein-Szanto et al., 1982) have been observed in the mouse epidermis treated with one tumor promoter TPA (12-o-tetradecanoylphorbol-13-acetate) (Klein-Szanto, 1984; Slaga and Klein-Szanto, 1983).

Reduction in coarseness of tonofibril bundles at some places (Fig. 12b) might suggest malformation of next higher cellular level of epidermis because in stratum spinosum the number of tonofilaments increases and, they aggregate into a coarse bundle, called tonofibrils (Skerrow and Skerrow, 1983). The compactness of these bundles is very much essential for the proper differentiation and development of further higher layer of epidermis.

Stratum granulosum is characterized by the presence of a large number of keratohyalin granules, which are not membrane bound but are free in the cytoplasm. Histidine rich proteins, too, have been identified in these granules (Murozuka et al., 1979; Lynley and Dale, 1983). These granular cells get abruptly transformed into cornified cells consisting of keratin filaments, interposed between which are keratohyalin derived interfilamentous matrix materials, which serve the function of aggregation of the keratin filaments. Stratum granulosum is characterized by the presence of small granules known by various names: Odland bodies, lamellated bodies, or

membrane-coating granules. Higher in epidermis, these granules increase in number and size, move toward the distal cell membrane, fuse with the plasmalemma, and release their contents into the intercellular space. It has been postulated that these granules are responsible for the thickening of the stratum corneum cells and formation of the stratum corneum barrier (Wolff_Schreiner, 1977; Thompson and Hunt, 1966). Reduction in the number of these granules (Fig. 11b), which can lead to poor barrier function.

In the epidermis, some cells are also present to perform specialized functions. Langerhans cells are important in recognizing the presence of antigens and facilitating an immune response. They are mostly found in upper spinous layer of epidermis. They are referred to as non-keratinocytes because they lack desmosomes and tonofilaments. They have long dendritic processes, which can traverse the intercellular space up to the granular cell layer (Rodriguez and Caorsi, 1967). The dendritic processes capture cutaneous antigens and send them to lymphocytes in the initiation of an immune response. There is significant reduction in the dendritic processes (Fig. 13b), which may be indicative of occurrence of some type of immune reaction in the skin due to the absorption of JP-8.

Binding to SC is an index of the relative affinity of the chemical for the solvent and SC. It plays a significant role in establishing the flux. Generally higher binding to SC leads to higher percutaneous absorption (Bronaugh et al., 1981). However, too much binding to SC, which is an indicative of lipophilicity, leads to lower dermal absorption. Hence, the unusual low percutaneous absorption of TET can be attributed to its very high binding to SC, which might be leading to depot formation in the SC. Others have reported similar findings. In one study of dermal absorption and distribution of topically dosed jet fuels, hexadecane absorption was found lower than DOD and NAP (Riviere et al., 1999). Moreover, one another study has reported lower percutaneous absorption of TET than TRI or undecane (McDougal et al., 2000). In our earlier work (Singh et al., 2001b), hexadecane was found to exhibit lower permeability coefficient than heptane or xylene, but got retained by the skin more than that of heptane or xylene. Comparatively larger molecular size of TET or hexadecane would have possibly played a role for their lesser transport in comparison to other chemicals in the above studies.

Jss depends on concentration of permeant in donor solution. Four μCi of each chemical was used in 1ml of donor solution, which were equivalent to 519.48 nmol/ml, 74.76 nmol/ml, 221 nmol/ml, 493.83 nmol/ml, and 470.58 nmol/ml of DOD, TRI, TET, NAP, and 2-MN, respectively, on the basis of their specific activity. TRI showed greater Jss even if it was present in the donor cell at comparatively low concentration (74.76 nmol/ml). Permeability coefficient is independent of concentration of permeant in the donor solution. Generally, higher permeability leads to higher percutaneous absorption. TRI exhibited higher permeability coefficient (Kp) value, which was also bound to SC more. The greater Kp of TRI may be described by its lower t_L and greater extraction of SC lipid and protein as suggested by FTIR findings. In this study, JP-8 has been used as vehicle because the five test chemicals are its components. Hence, the permeability coefficient of pure test chemicals would be different than from JP-8 mixture. JP-8, being mixture of several chemicals, might have influenced the absorption of these chemicals.

Diffusion coefficient is a function of the individual permeant molecules, which depends on size and nature of permeant molecules and the media through which they are diffusing. NAP being of smaller size diffuses at greater rate than 2-MN, although both are having comparable binding to SC (Table 6). TRI is larger in size in comparison to the size of NAP, but exhibit greater D because its binding to SC is greater than that of NAP.

Fig. 15 shows the relationship between permeability and diffusion coefficient values. Permeability coefficient values are well correlated with diffusion coefficient values ($r^2 = 0.9949$). However, there was not a good correlation ($r^2 = 0.1037$) between partition and permeability coefficient (figure not shown). Hence, higher permeability of TRI or NAP can be ascribed to their higher diffusion coefficient. NAP being of smallest molecular weight gets transported well, which is also supported by its higher diffusion coefficient value.

TEWL is widely used to characterize the macroscopic changes in the barrier properties of skin; a high TEWL generally indicates barrier perturbation. Several investigators (Elias, 1983; Wertz and Downing, 1982) have suggested that the high resistance of the SC to water flux is due to the extended multilamellar lipid domains present intercellularly in the SC. Accordingly, molecules must traverse the hydrocarbon regions of these lamellae in order to diffuse across this barrier. It

is generally accepted that a solvent, such as ethanol, removes intercellular material, which results in cutaneous barrier disruption (Scheuplein and Blank, 1971). Hence, an increased TEWL through the skin is due to the corresponding increase in the lipid extraction by the test chemicals (Table 7 and table 8), which is supported by FTIR findings.

We have estimated the amount of chemicals absorbed on the basis of their steady state flux and their percentage concentration in JP-8, assuming both hands (0.25 m^2 surface area) exposed for 8 h. Both hands can be in contact with JP-8 during foam removal in the fuel tank of jet engine. Other modes of JP-8 exposure are also probable as has been mentioned in introduction. The surface area of 0.25 m^2 is purely assumption. It may be less or more and accordingly amount of chemicals absorbed would vary. The amount of chemicals absorbed is directly proportional to surface area of skin exposed with chemicals. We have adjusted the experimentally determined flux for the actual proportion of individual chemical in JP-8. The usual proportion of chemicals in JP-8 are 4.7%, 4.4%, 3.0%, 1.1%, and 1.5% for DOD, TRI, TET, NAP, and 2-MN, respectively. The amount of chemical absorbed has been estimated more for TRI, which is due to its greater flux and permeability coefficient.

Skin regulates the body temperature. Any barrier perturbation may lead to increase in temperature (Thiele and van Senden, 1966). JP-8 has been implicated in skin barrier perturbation due to extraction of lipids and proteins from SC (Singh and Singh, 2001b). Hence, the test chemicals increased the temperature. TRI caused greater increase in temperature because of its greater ability of extracting lipid and protein from SC.

As long as horny layer (SC) is intact, capacitance should not be influenced by the increase in the amount of tissue fluid contained beneath the SC. Even a small scratched wound in the test area, which exposed the underlying living tissue, results in a marked increase in capacitance (Tagami et al., 1980). Hence, all the test chemicals increased capacitance because water from viable epidermis might have rushed up due to perturbed barrier. This is supported by higher increase in capacitance with TRI.

There is a relationship between insensible and sensible water loss by skin and influence of ambient and local temperatures on the responses of the sweat glands (Hemels, 1970). Since, we performed experiments under controlled room temperature and humidity; we do not expect an increase in TEWL on this account. In certain cases, the TEWL tends to increase with increasing capacitance. A possible reason for this could be an increase in skin moisture, induced by occlusion, which is also known to reduce diffusional resistance of the SC (Marie et al., 1992). A lack of correlation between TEWL and the hydration status of the SC has also been reported (Triebskorn et al., 1983). We found increase in TEWL for all of the chemicals due to rupture of skin barrier and increase in temperature. Water loss by skin is thought to be a temperature dependent diffusion phenomenon through a water barrier located in horny layer (Tthiele and Malten, 1973). There was no significant ($p<0.05$) increase in TEWL for control at different time points. Moreover, we subtracted the TEWL of control sites from the corresponding test sites. Hence, increase in TEWL can not be attributed to occlusion effect.

Irritation tends to reduce the efficiency of the SC barrier function. We found perturbation in macroscopic barrier as evidenced by significant ($p<0.05$) increase in temperature, capacitance, and TEWL at test sites, in comparison to control, immediately after chemically saturated patch-removal. Diffusibility of a chemical substance through the SC is an important factor affecting irritation which depends on a complex interaction of variables; temperature, degree of hydration, physical properties of the penetrating substance, and damage to the structural or chemical integrity of the SC membrane itself (Mathias and Maibach, 1978). Diffusibility through a membrane increases as the temperature of the membrane increases (Rothenberg et al., 1977). Increasing the water content of the SC (membrane hydration) as indicated by higher capacitance values generally enhances percutaneous absorption. JP-8 components have been found to extract SC lipids and proteins (Singh and Singh, 2002) resulting in damage to chemical integrity of the SC. Therefore, all of the JP-8 components caused moderate to severe erythema and edema.

Light microscopy provides visual evidences of the microscopic changes in the skin. We observed significant increase in epidermal thickness and detachment of SC at some places, which indicates perturbation of SC barrier properties (Fig 21a and b). The dermis, a critical organ of the body, not only provides the nutritive, immune, and other support systems for the epidermis through a

thin papillary layer adjacent to the epidermis but also plays a role in temperature, pressure, and pain regulation. The dermis consists of collagenous fibers (70%), and elastic connective tissue, in a semigel matrix of mucopolysaccharides (Roberts and Walters, 1998). In the chemically treated skin samples (Fig. 22a, b, c, and d) collagen fibers' bundles were found comparatively shortened. TRI decreased CL more than others because it is more permeable to skin. Since TET binds with SC and virtually forms a depot, therefore, it would reach to the dermis in comparatively lesser amount. We found greater increase (recovery) in CL after 24 h of patch removal in case of TET than other chemicals. In control, the collagen fibers were bundled together and hence, appeared coarse and aggregated (Fig. 22a). In treated skin, collagen fibers' bundles were found shortened less coarse and rarefied (Fig. 22b and c). These changes in collagen fibers' bundle due to dermal absorption of JP-8 components may lead to dermatotoxicity.

The main cells present in the dermis are fibroblasts, which produce the connective tissue components of collagen, laminin, fibronectin and vitronectin; mast cells, which are involved in the immune and inflammatory responses; and melanocytes, involved in the production of the pigment melanin (Roberts and Walters, 1998). Fig. 20 showed fewer fibroblasts in control skin. However, Fig.22b showed a greater number of fibroblasts in TRI treated skin than the control, which suggests some kinds of immune reaction and inflammatory processes caused by it (Ulrich, 1999; Ulrich and Lyons, 2001; Singh and Singh, 2001a).

4. RFERENCES

Bhatia K, Singh, J., 1998. Mechanism of transport enhancement of LHRH through porcine epidermis by terpenes and iontophoresis: Permeability and lipid extraction studies. *Pharm. Res.* **15,** 1857-1862.

Bommannan, D.B., Potts, R.O., Guy, R.H., 1991. Examination of the effect of ethanol on human SC *in vivo* using infrared spectroscopy. *J. Control. Rel.* **16,** 299-304.

Breathnach, A.S., 1971. An Atlas of Ultrastructure of Human Skin: Development, Differentiation and Post-natal Features, J. A. Churchill, London.

Bronaugh, R.L., Collier, S.W., 1991. *In vitro* percutaneous absorption. F.N. Marzulli and H.I. Maibach (edts.). *Dermatotoxicology*, Hemisphere Publishing Corporation, NY, 61-73.

Draize, J.H., Woodard, G., Calvery, H.O., 1944. Methods for the study of irritation and toxicity of substances applied topically to the skin and mucous membranes. *J. Pharmacol. Exp. Ther.* **82,** 377-390.

Elias, P.M., 1983. Epidermal lipids, barrier function, and desquamation. *J. Invest. Dermatol.* **80(Supple.),** 44s-49s.

Elias, J.J., 1989. The Microscopic Structure of the Epidermis and its Derivatives. In: *Percutaneous Absorption: Mechanism – Methodology – Drug Delivery,* R.L. Bronaugh and H.I. Maibach, (edts.). 2nd edition, Marcel Dekker, Inc.

Environmental Protection Agency, 1989. *Risk Assessment Guidance for Superfund, Vol 1, Human Health Evaluation Manual,* Part A, Interim final, Washington, D.C.: Office of the Emergency and Remedial Response, EPA/ 540/ 1-89/ 002.

Goates, C.Y., Knutson, K., 1994. Enhanced permeation of polar compounds through human epidermis. I. Permeability and membrane structural change in the presence of short-chain alcohols. *Biochim. Biophys. Acta.* **1195,** 169-179.

Grant, G.M., Jackman, S.M., Kolanko, C.J., Stenger, D.A., 2001. JP-8 jet fuel-induced DNA damage in H4IIE rat hepatoma cells. *Mutat. Res. Genet. Toxicol. Environ. Mutag.* **490,** 67-75.

Grant, G.M., Shaffer, K.M., Kao, W.Y., Stenger, D.A., Pancrazio, J.J., 2000. Investigation of *in vitro* Toxicity of jet fuels JP-8 and Jet A. *Drug Chem. Toxicol.* **23,** 279-291.

Gray, G.M., Yardley, H.J., 1989. Lipid composition of cells isolated from pig, human, and rat epidermis, *J. Lip. Res.* **16,** 434.

Harris, D.T., Sakiesrewa, D., Robledo, R.F., Young, R.S., Witten M., 2000. Effects of long term JP-8 jet fuel exposure on cell mediated immunity. *Toxicol. Ind. Health* **16,** 78-84.

Hayton, W.L., Chen, T., 1982. Correction of Perfusate Concentration for Sample Removal. *J. Pharm. Sci.* **71,** 820-821.

Hemels, H.G.W.M., 1970. The effect of propanolol on the acetylcholine-induced sweat gland response in atopic and non-atopic subjects. *Br. J. Dermtol.* **83,** 312-314.

Humasons, G.L., 1972. *Animal Tissue Techniques,* 3rd edition, pp. 7, 45-47, 156-158. W. H. Freeman and Company, San Francisco.

Hurst, L.N., Brown, D.H., Murray, K.A., 1984. Prolonged life and improved quality for stored skin graft. *Plast. Reconstr. Surg.* **73,** 105-109.

Idson, D.R., 1978. *In vivo* measurement of transepidermal water loss. *J. Soc. Cosmet. Chem.* **29,** 573-580.

Kai, T., Isami, T., Kurosaki, Y., Nakayama, T., Kimura, T., 1993. Keratinized epithelial transport of beta blocking agents. II. Evaluation of barrier property of stratum corneum by using model lipid system. *Biol. Pharm. Bull.* **16,** 284-287.

Klein-Szanto, A.J., Nettesheim, P., Saccomanno, G., 1982. Dark epithelialcells in preneoplastic lesions of the human respiratory tract. *Cancer* **1,** 107-113.

Klein-Szanto, A.J.P., 1984. Morphological Evaluation of Tumor Promoter Effects on Mammalian Skin in Mechanism of Tumor Promotion, Tumor Promotion and Skin Carcinogenesis, Vol. II, T.J. Slaga, (ed.). CRC Press, Boca Raton, FL.

Kligman, A.M., Christophers, E., 1963. Preparation of isolated sheets of human SC. *Arch Dermato.* **88,**702-705.

Koenig, J.L., Snively, C.M., 1998. Fast FTIR Imaging: Theory and Applications. *Spectroscopy.* **11,** 22-28.

Lavker, R.M., Sun, T., 1982. Heterogeneity in epidermal basal keratinocytes: morphological and functional correlations. *Science* 215, 1239-.

Lavker, R.M., Sun, T.T, 1983. Epidermal stem cells. *J. Invest. Dermatol.* **81,** 121s-127s.

Lazo, N.D., Maine, J.G., Downing, D.T., 1995. Lipids are covalently attached to rigid corneocyte protein envelopes existing predominantly as β-sheets: a solid-state nuclear magnetic resonance study. *J Invest Dermatol.* **105,** 301-313.

Luna, L.G., 1968. *Manual of Hstologic Staining Methods of the Armed Forces Institute of Pathology*, 3rd ed., McGraw-Hill, New York.

Lynley, A.M., Dale, B.A., 1983. The Characterization of Human Epidermal Filaggrin: a Histidine-rich Keratin filament-aggregating protein. *Biochim. Biophys. Acta* **1,** 28-35.

Marie, L., Hakan, O., Tony, A., Ylva, W.L., 1992. Friction, capacitance and transepidermal water loss (TEWL) in dry atopic and normal skin. *British J. Dermatol.* **126,** 137-141.

Mathias, C.G., Maibach, H.I., 1978. Dermatotoxicology monographs I. Cutaneous irritation: factors influencing the response to irritants. *Clin. Toxicol.* **13,** 333-346.

Mattie, D.R., Alden, C.L., Newell, T.K., Gaworski, C.L., Flemming, C.D., 1991. A 90-day continuous vapor inhalation toxicity study of JP-8 jet fuel followed by 20 or 21 months of recovery in Fischer 344 rats and C56BL/6 mice. *Toxicol. Path.* **2,**77-87.

McDougal, J.N. Jepson G.W., Clewell, H.J.III, McNaughton, M.G., Anderson, M.E., 1986. A physiological pharmacokinetic model for dermal absorption of vapors in the rat, *Toxicol. Appl. Pharmacol.* **85,** 286-294.

McDougal, J.N., Jepson, G.W., 1990. Dermal absorption of organic chemical vapors in rats and humans. *Fundam. Appl. Toxicol.* **14,** 299-308.

McDougal, J.N., Pollard, D.L., Weisman, W., Garrett, C.M., Miller, T.E., 2000. Assessment of Skin Absorption and Penetration of JP-8 Jet Fuel and Its Components. *Toxicol. Sci.* **55,** 247-255.

Monteiro-Riviere, N.A., Stromberg, M.W., 1985. Ultrastructure of the integument of the domestic pig (Sus scrofa) from one through fourteen years of age, *Anat. Histol. Embryol.* **14,** 97-115.

Monteiro-Riviere, N.A., 1991. Comparative Anatomy, Physiology, and Biochemistry of Mammalian Skin in Dermal and Ocular Toxicology: Fundamental and Methods, David W. Hobson, Ed., CRC Press Inc.

Murozuka, T., Fukuyama, K., Epstein, W.L., 1979. Immunochemical Comparision of Histidine-rich Protein in Keratohyalin Granules and Cornified Cells. *Biochim. Biophys. Acta* **2,** 334-345.

Riviere, J.E., Brooks, J.D., Monteiro-Riviere, N.A., Budsaba, K., Smith, C.E., 1999. Dermal Absorption and Distribution of Topically Dosed Jet fuels Jet-A, JP-8, and JP-8 (100). *Toxicol. Appl. Pharmacol.* **160,** 60-75.

Roberts, M.S., Walters, K.A., 1998. The relatioship Between Structure and Barrier Function of Skin. In *Dermal Absorption and Toxicity Assessment.* M.S. Roberts and K. A. Walters, (eds.). pp. 1-42, Marcel Dekker, Inc., New York.

Robledo, R.F., Barber, D.S., Witten, M.L., 1999. Modulation of bronchial epithelial cell barrier function by *in vitro* jet propulsion fuel 8 exposure. *Toxicol. Sci.* **51,** 119-125.

Rodriguez, E.M., Caorsi, I., 1967. A Second Look at the Ultrastructure of the Langerhans Cell of the Human Epidermis. *J. Ultrastruct. Res.* **3,** 279-284.

Rosenthal, D.S., Cynthia, M.G., Simbulan-Rosenthal, C.M.G., Liu, W.F., Stoica, B.A., Simulson, M.E., 2001. Mechanism of JP-8 Jet Fuel Cell Toxicity. II. Induction of Necrosis in skin fibroblasts and keratinocytes and Modulation of Levels of Bcl-2 Family Members. *Toxicol. Appl. Pharmacol.* **171,** 107-116.

Rothenberg, H.W., Menne, T., Sjolin, K.E., 1977. Temperature dependent primary irritant dermatitis from lemon perfume. *Contact Dermatitis* **3,** 37-48.

Scheuplein, R.J., Blank, I.H., 1971. Permeability of the skin. *Physiol. Rev.* **4,** 702-747.

Scheuplein, R.J., 1978. Skin as a barrier; in the Physiology and Pathophysiology of skin. A. Jaret, (ed.). Academic Press, New York, **5,** 1693-1730.

Singh, S., Singh, J., 2001a. Effect of JP-8 jet fuel Exposure on the Ultrastructure of Skin. *J. Toxicol.-Cut. & Ocular Toxicol.* **20,** 11-21.

Singh, S., Singh, J., 2001b. Dermal toxicity: effect of jet propellant-8 fuel exposure on the biophysical, macroscopic and microscopic properties of porcine skin. *Environ. Toxicol. Pharmacol.* **10,** 123-131.

Singh, S., Zhao, K., Singh, J., 2002. *In vitro* permeability and binding of hydrocarbons in pig ear and human abdominal skin. *Drug Chem. Toxicol.* **25,** 83-92.

Skerrow, D., Skerrow, C.J., 1983. Tonofilament differentiation in human epidermis: isolation and polypeptide chain composition of keratinocyte subpopulations. *Exp. Cell Res.* **1,** 27-35.

Slaga, T.J., Klein-Szanto, A.J.P., 1983. Initiation-promotion versus complete skin carcinogenesis in mice: importance of dark basal keratinocytes (stem cells). *Cancer Invest.* **1,** 425-36.

Steven, A.C., Bisher, M.E., Roop, D.R., Steinert, P.M., 1990. Biosynthetic pathways of filaggrin and loricrin-two major proteins expressed by terminally differentiated mouse keratinocytes. *J. Struct. Biol.* **104,** 150-162.

Tagami, H., Ohi, H., Iwatsuki, K., Kanamaru, Y., Yamada, M., Ichijo, B., 1980. Evaluation of the skin surface hydration *in vivo* by electrical measurement. *J. Invest. Dermatol.* **75,** 500-507.

Thiele, F.A.J., van Senden, K.G., 1966. Relationship between skin temperature and the insensible perspiration of the human skin. *J. Invest. Derm.* **47,** 307-312.

Thiele, F.A.J., Malten, K.E., 1973. Evaluation of the skin damage I. *Br. J. Dermatol. 89,* 373-382.

Thompson, S.W., Hunt, R.D., 1966. Selected Histochemical and Histopathological Methods. Charles C Thomas, Springfield, II, p. 51.

Triebskorn, A., Gloor, M., Greiner, F., 1983. Comparative investigations on the water content of the stratum corneum using different methods of measurement. *Dermatologica* **167,** 64-69.

Ulrich, S.E., 1999. Dermal Application of JP-8 jet fuel induces Immune Suppression. *Toxicol. Sci.* **52,** 61-67.

Ulrich, S.E., Lyons, H.J., 2000. Mechanisms Involved in the Immunotoxicity Induced by Dermal Application of JP-8 jet fuel. *Toxicol. Sci.* **58,** 290-298.

Wertz, P.W., Downing, D.T., 1982. Glycolipids in mammalian epidermis: structure and function in the water barrier. Science **217,** 1261-1262.

Wester, R.C., Melendres, J., Sarson, R., McMaster, J., Maibach, H.I., 1991. Glyphosate Skin Binding, Absorption, Residual Tissue Distribution, and Skin Decontamination. *Fundam. Appl. Toxicol.* **16,** 725-732.

Wolff-Schreiner, E., 1977. Ultrastructural cytochemistry of the epidermis. *Int. J Dermatol.* **2,** 77-101.

Yamane, M.A., Williams, A.C., Barry, B.W., 1995. Effects of terpenes and oleic acid as skin penetration enhancers towards 5-fluorouracil as assessed with time, permeation, partitioning and differential scanning calorimetry. *Int. J. Pharm.* **116,** 237-251.

Zhao, K., Singh, J., 2000. Mechanism(s) of *In Vitro* Percutaneous Absorption Enhancement of Tamoxifen by Enhancers. *J. Pharm. Sci.* **6,** 771-780.

6. RESEARCH EXPERIENCE:

This DEPSCoR award provided research experience to a research associate, a graduate student and two professional (Pharm.D.) students.

7. PEER-REVIEWED PUBLICATIONS AND PRESENTATIONS:

Publications:

1. Somnath Singh and Jagdish Singh, Percutaneous absorption, biophysical, and macroscopic barrier properties of porcine skin exposed to major components of JP-8 jet fuel. Environmental Toxicology and Pharmacology, 14, 77-85, 2003.

2. Somnath Singh, Kaidi Zhao and Jagdish Singh, *In vivo* percutaneous absorption, skin barrier Perturbation and irritation from JP-8 jet fuel components. Drug and Chemical Toxicology, 26, 135-146, 2003.

3. Somnath Singh and Jagdish Singh, Dermal toxicity and microscopic alterations in vivo in rabbit by components of JP-8 jet fuel, Environmental Toxicology and Pharmacology, Accepted, 2003.

4. Somnath Singh, Kaidi Zhao, and Jagdish Singh, In vitro permeability and binding of hydrocarbons in pig ear and human abdominal skin. Drug and Chemical Toxicology, 25(1), 83-92, 2002.

5. Somnath Singh and Jagdish Singh, Effect of JP-8 jet fuel exposure on the ultrastructure of skin. Journal of Toxicology- Cutaneous and Ocular Toxicology, 20, 11-21, 2001.

6. Somnath Singh and Jagdish Singh, Biophysical, macroscopic and microscopic changes in porcine skin due to JP-8 exposure. Environmental Toxicology and Pharmacology, 10, 123-131, 2001.

Presentations in National/International Symposia:

1. S Singh and J singh, Percutaneous absorption of model aliphatic and aromatic solutes. presented at the 28th International Symposium on Controlled Release of bioactive materials, San Diego, USA, June 24-27, 2001.

2. S. Singh and J Singh, Percutaneous absorption and binding to stratum corneum of model aliphatic and aromatic components of JP-8 jet fuel. Presented at AAPS Annual Meeting and Exposition, Denver, Colorado, October 21-25, 2001.

3. S. Singh and J. Singh. Skin barrier perturbation, irritation, and microscopic alterations *in vivo* in rabbit from JP-8 jet fuel. Presented at the 2002 AAPS Annual Meeting and Exposition, in Toronto, Ontario, Canada on November 10-14, 2002.

4. Somnath Singh and Jagdish Singh, Percutaneous absorption, biophysical, macroscopic, and microscopic barrier perturbation from six major components of JP-8 jet fuel. Presented at JP-8 Conference, Tucson, Arizona, January 10-12, 2001.

5. J Singh and S Singh, Effect of naphthalene and 1-methylnaphthalene on biophysical, macroscopic and microscopic properties of skin. Presented at Pharmaceutical congress of Americas, Orlando, FL, March 24-29, 2001. Abstract # 2300, p. 118.

6. S Singh and J Singh, Effect of aliphatic constituents of JP-8 on skin lipid and protein biophysics, and in vitro transepidermal water loss. Presented at Pharmaceutical congress of Americas, Orlando, FL, March 24-29, 2001. Abstract # 2301, p. 118.

7. J Singh and S Singh, Effect of JP-8 on the biophysical, macroscopic and microscopic properties of the skin. presented at annual AAPS meeting, Indianapolis, October 29-November 2, 2000.

8. S Singh, K Zhao, and J Singh, Pig skin as model for humans to study in vitro percutaneous absorption of chemicals. presented at annual AAPS meeting, Indianapolis, October 29-November 2, 2000.

9. S Singh, and J Singh, Ultrastructural changes in the porcine skin due to JP-8 exposure. Presented at annual AAPS meeting, Indianapolis, October 29-November 2, 2000.

10. J Singh, K Zhao, and S Singh, Barrier function and irritation from chemicals in vivo in weanling pigs. Presented at annual AAPS meeting, Indianapolis, October 29-November 2, 2000.